IDŐJÁRÁS

QUARTERLY JOURNAL
OF THE HUNGARIAN METEOROLOGICAL SERVICE

CONTENTS

VOL. 98 * NO. 3 * JULY–SEPTEMBER 1994

IDŐJÁRÁS

Quarterly Journal of the Hungarian Meteorological Service

Editor-in-Chief
E. MÉSZÁROS

Editor
T. TÄNCZER

Technical Editor
Mrs. M. ANTAL

Editorial Office: P.O. Box 39, H–1675 Budapest

Subscription from customers in Hungary should be sent to the Financial Department of the Hungarian Meteorological Service Kitaibel Pál u. 1, 1024 Budapest. The subscription rate is HUF 2000.

Abroad the journal can be purchased from the distributor: KULTURA, P.O. Box 149, H–1389 Budapest. The annual subscription rate is USD 56.

IDŐJÁRÁS

Quarterly Journal of the Hungarian Meteorological Service
Vol. 98, No. 3, July–September 1994

Experimental study on low-pressure aerosol filtration through fibrous filters

M. Attoui[1], **A. Renoux**[1], **C. Vauge**[2] and **D. Boulaud**[3]

[1] *Laboratoire de Physique des Aérosols et de Transfert des Contaminations, Université Paris XII, Avenue du Général de Gaulle, 94010 Creteil, France*
[2] *Laboratoire d'Instrumentation Physique, Université Paris XII*
[3] *CEA/IPSN/DPEI/SERAC/LPMA, Saclay, France*

(Manuscript received 21 June 1994; in final form 25 July 1994)

Abstract—This work concerns the efficiency of fibrous filters in the 'transition-flow regime'. We used filters with a mean fibre diameter of 2.7 μm, and a packing density, α, of 0.008, in a pressure range from 50 to 1000 hPa. Electrostatic classification was used to generate particles with a size distribution from 0.04 to 0.3 μm. The penetration was measured at a flow rate of 40 cm s^{-1}. Experimental results showed that the penetration decreased with pressure, while we also observed that the maximum penetration size shifted to larger particle sizes.

Key-words: aerosol, filtration, low pressure.

1. Introduction

When investigating, for instance, aerosol influence on the atmospheric radiative balance (*Lenoble*, 1993), it becomes more and more necessary to collect atmospheric particles at high altitude; consequently corresponding to low pressure. However, filtration models established for pressures close to atmospheric pressure, may no longer be valid. This is what prompted us to study the behaviour at low pressures of usual filters, down to one hectopascal.

Let us recall that the captation efficiency, E, of a filter is defined as the ratio of the number of retained particles to the number of incoming particles, i.e.:

$$E = (N_{up} - N_{do})/N_{up},$$

where N_{up} is the upstream particle concentration, and N_{do} the corresponding downstream one.

The penetration coefficient, P, is often preferentially used, defined as follows:

$$P = 1 - E = N_{do}/N_{up}.$$

The flow around the fibre, on which (among other factors) the penetration depends, is characterised by a dimensionless coefficient Kn, the Knudsen number of a fibre; defined as the ratio of twice the free mean path of the molecules of carrier gas, λ, to the fibre diameter, D_f:

$$Kn = 2\lambda/D_f.$$

According to the *Devienne* classification (1958), the flow regime can be subdivided into several domains:

1°– $Kn < 0.001$	Continuous flow regime
2°– $0.001 < Kn < 0.25$	Continuous flow regime with gas slip effect
3°– $0.25 < Kn < 10$	Transition flow regime
4°– $Kn > 10$	Molecular flow regime.

Our investigation is defined in the transition flow regime, or Knudsen regime, i.e. for Kn numbers ranging from 0.25 and 10, because very little work has been carried out so far within this field.

Actually, previous studies on low pressure filtration are scarce, be they theoretical or experimental. *Kirsch* and *Stechkina* (1978), and *Manson* (1984, 1988) have carried out studies, within the transitional flow regime, on the resistance (pressure drop) of a flow through a fibrous filter. *Zhang* and *Liu* (1992) have made experimental measurements of fibrous filter efficiencies in the pressure range of 1000 hPa–100 hPa.

2. *Experimental study and theory*

The classical method, illustrated in *Fig. 1*, involves sampling aerosols from a flow passing through the filter with both an upstream and a downstream concentration, and measuring those by means of a condensation nuclei counter (CNC).

However, this method can no longer be used when working at sub-atmospheric pressures. In fact, the loss in pressure would induce, more or less, rapid evaporation of the alcohol contained in the CNC saturator, and this would be drawn into the CNC—except model 3760 from T.S.I., which possesses a pressure equalization tube and can only operate correctly down to 100 hPa. This

counter has a further drawback of working solely with low particulate concentrations.

We subsequently developed an original method, allowing operation down to 10 hPa, in order to combat these restrictions (*Attoui et al.*, 1993a, b; *Attoui*, 1994).

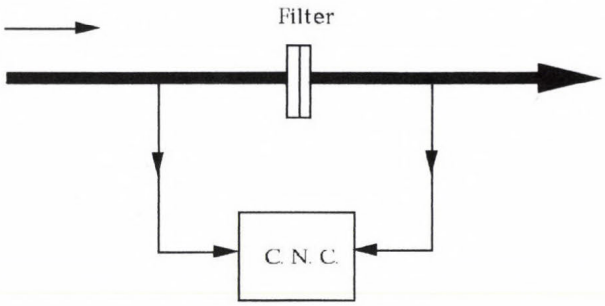

Fig. 1. Classical method for filter penetration measurement.

2.1 Principle of the method

An aerosol-loaded air flow is sent through the filter under study, being driven by a pressure gradient from one side of the filter to the other. This pressure gradient decreases exponentially and reaches zero after a relatively short time (*Fig. 2*).

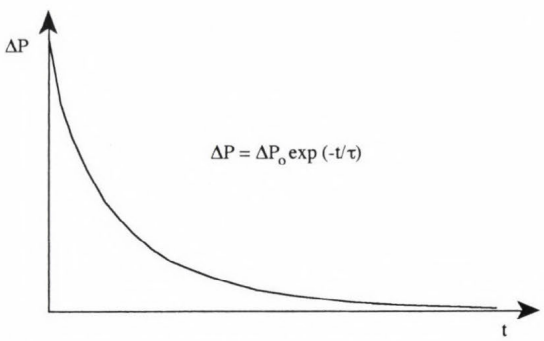

Fig. 2. Decrease in the pressure difference undergone by the filter.

This pressure gradient corresponds to an air velocity, which reaches zero at the same time as Δp. Every studied pressure possesses such a gradient. Those decreasing pressure gradients are obtained by emptying a tank into another through a cylindrical pipe, the whole set remaining totally isolated from the outside. For this purpose, two tanks (I and II) of equal volume are to be used, initially at different pressures P_1 and P_2. Their pressures reach an equilibrium value through the filter after opening the valve, V_a, as shown in *Fig. 3*.

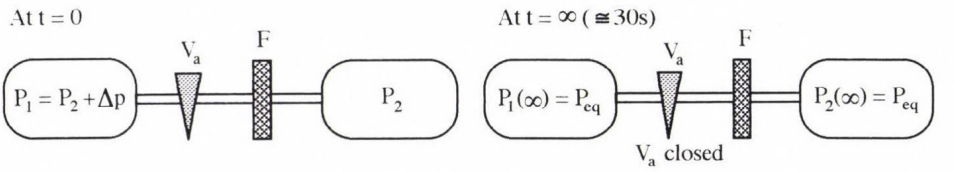

Fig. 3. Pressure in the two tanks at time, $t = 0$, and at equilibrium.

If we operate in laminar regime, the pressure difference, $\Delta p(t) = p_1(t) - p_2(t)$, decreases according to the exponential relationship:

$$\Delta p\,(t) = \Delta p\,(0)\,\exp\left[-\frac{t}{\tau}\right], \tag{1}$$

where τ is given by:

$$\tau = \frac{VM}{2KRT},$$

and R is the universal gas constant; T is the absolute temperature for the system; V is the volume of both tanks; K is the circuit resistance to flow. The derivation of the above relationship may be found in Appendix 1. Eq. (1) may also be written in terms of the flow velocity, as follows.

For this pressure gradient there corresponds a shift of matter, dm_1, from tank I towards tank II:

$$dm_1 = K\,[p_1(t) - p_2(t)]\,dt,$$

but:

$$dm_1 = \rho v s\,dt,$$

where ρ is the specific mass of the fluid (air); v is the flow velocity; s is the cross-sectional area of the fluid path.

$$\rho v s\,dt = K\Delta p = K\Delta p(0)\,e^{-t/\tau}\,dt,$$

hence:

$$v = \left[\frac{K\Delta p(0)}{\rho s}\right] e^{-t/\tau}.$$

Let us consider:

$$v_0 = \left[\frac{K\Delta p(0)}{\rho s}\right].$$

Thus v becomes:

$$v = v_0 e^{-t/\tau}. \tag{2}$$

2.2 Determination of the variation in air mass difference between tanks I and II as a function of time

The filter 'works' during transfer with a mean efficiency, $\bar{E}$, which may be approximated to $E(v_0)$. We only need to isolate the two tanks after the pressures are balanced by shutting valve, V_a, returning to atmospheric pressure by injecting clean nitrogen through an ULPA filter. It is then possible to count the number of particles having flowed through the filter and those remaining in the second tank, using the CNC at atmospheric pressure. The number of particles upstream of the filter is determined from the known mass concentration in tank I, under pressure p_1, and from the mass transferred, m. So that:

$$N_{up} = C_{m,p\,(up)} m,$$

where $C_{m,p}$ is the mass concentration of aerosol at pressure, p, given by:

$$C_{m,p\,(up)} = C_{m,P_{atm}^{(up)}} \times \frac{p}{p_{atm}}.$$

With $C_{m,P_{atm}^{(up)}}$ being the mass concentration of aerosol at atmospheric pressure in the upstream tank. The mass of gas transferred from tank I to tank II, m, is given by Eq. (3) below. Appendix 2 shows the derivation of this relationship.

$$m = \frac{VM}{2RT} \Delta P_0, \tag{3}$$

where ΔP_0 is the difference of pressures between tanks I and II at $t = 0$.

3. Experimental set-up

Our experimental set-up, shown in *Fig. 4*, consists of three distinct parts. The first of these is the generator system, composed of an atomizer, a dryer, a neutralizer and an electrostatic classifier. The second part is the testing bench, comprising of two stainless steel tanks of equal volume (20 litres) connected by a 70 cm long, 6 mm inside diameter stainless steel pipe. They are mounted on a support, which also contains:

— a filter holder, F, and a pneumatic valve, V_a, electrically operated to allow the air flow between the two tanks, or to isolate one from the other;

— a vacuum pump capable of evacuating both of tanks at the same time or separately, by means of manual valves, and equipped with a filter and a safety-check valve for oil vapour;
— a manometer on each of the two tanks, connected via a data processing card to a PC, and to a direct readout.

The final part is the counting system, consisting of a personal computer (PC) and a condensation nucleus counter (CNC). With the appropriate software, and use of the data processing card, particles may be counted one by one using the pulses issued by the CNC and collected by the card. This gives us a direct count of the number of particles having flowed through the filter.

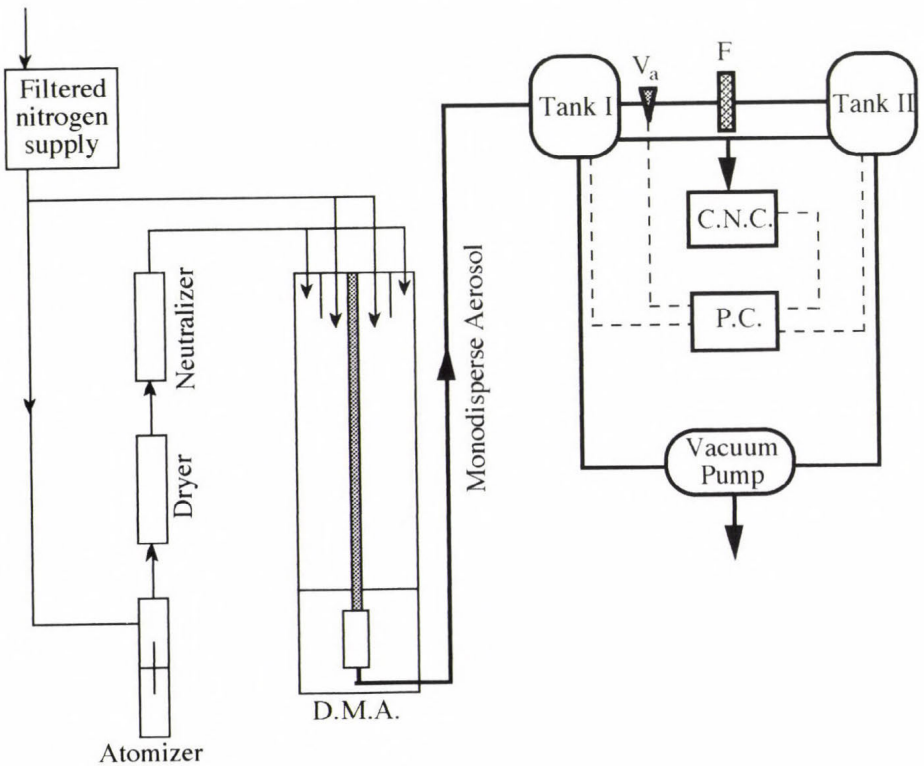

Fig. 4. Experimental set-up.

4. Experimental results

We tested 'formettes' (glass fibre filters) from *B. Dumas* company, at different pressures. The mean fibre diameter was 2.7 μm and the filter thickness was 0.3 mm. *Fig. 5* shows the variation in the particle number concentration

plotted as a function of pressure, for particles of 0.1 μm diameter in either of the other tanks. The relationship given by the equation:

$$C_{(p)} = C_{P_{atm}} \left[\frac{p}{p_{atm}} \right],$$

was confirmed by our results, so by measuring $C_{p_{atm}}$, we can easily go down to $C_{(p)}$.

Fig. 6 gives the variation of penetration, *P,* as a function of pressure, from 1000 hPa down to 50 hPa, for a filtration speed of 40 cm s^{-1}.

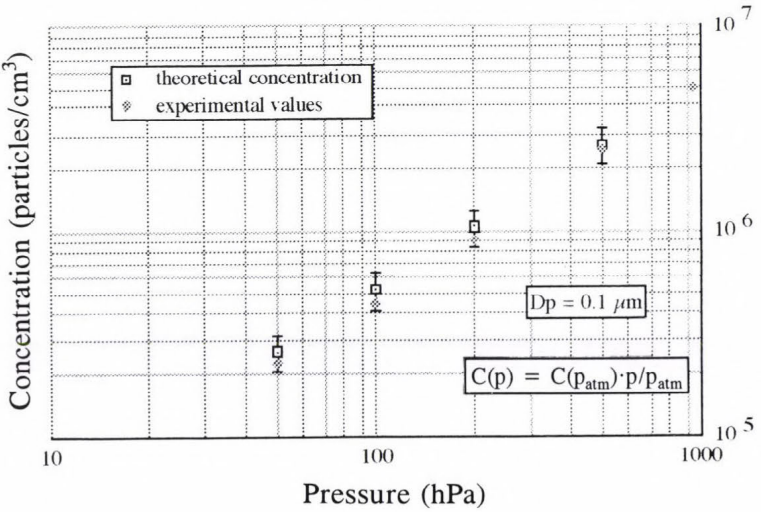

Fig. 5. Variation of the particle volumetric concentration as a function of pressure.

Fig. 7 illustrates the variation of penetration, *P,* as a function of the particle diameter, D_p, obtained for differing pressure conditions. As shown, six particulate diameters were studied: 0.04, 0.06, 0.1, 0.15, 0.2, and 0.3 μm.

5. Conclusion

Our first experimental readings clearly showed that the penetration, *P,* of a filter decreases significantly with pressure; i.e. when the Knudsen number of a filter increases.

We also noticed a slight shift of maximum penetration values towards the larger aerosol diameters, as already pointed out by *Zhang* and *Liu* (1992).

As a continuation of this work, we intend to carry out the same experiments at filtration speeds 10 times lower. A first comparison of our experimental results with the theory developed by *Payet* (1992), from *Rubow* works (1981), appears to give satisfactory results.

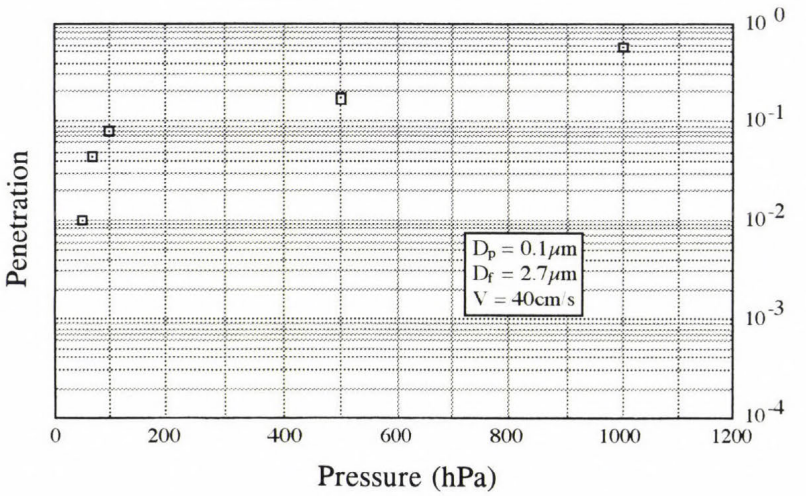

Fig. 6. Variation of penetration as a function of pressure for a given diameter.

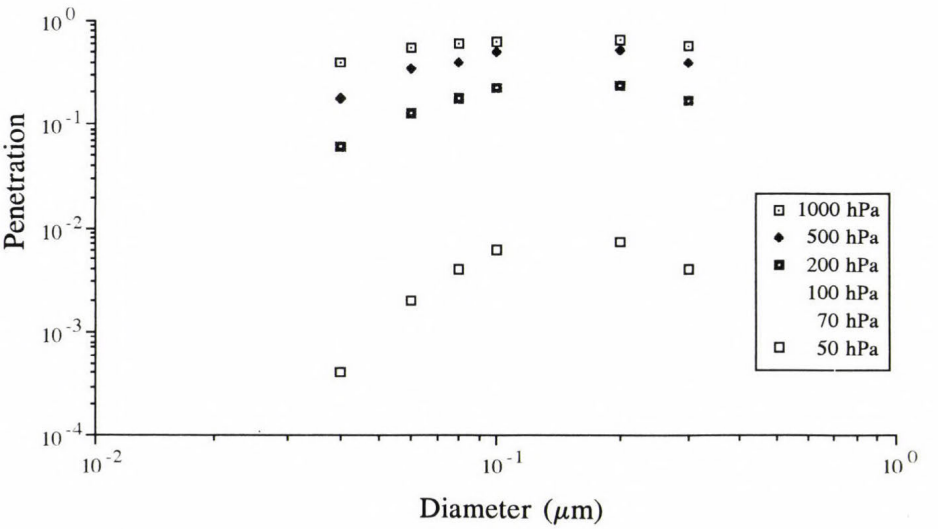

Fig. 7. Spectral variation of penetration for several pressures.

References

Attoui, M., Renoux, A. and *Madelaine, G.*, 1993a: Etude experimentale sur la filtration des aérosols par les filtres à fibres à basse pression. *COFERA Actes 1993.* GAMS, Paris.

Attoui, M., Renoux, A. and *Boulaud, D.*, 1993b: Fibrous filters efficiency in low pressure conditions. *Journal of Aerosol Science 24*, 37-39.

Attoui, M., 1994: *Une nouvelle approche experimentale de la mesure de l'efficacité des filtres à fibres à basse pression.* Thèse en science des aérosols, Université Paris XII.

Comolet, R., 1976: *Mécanique expérimental des fluides*. Masson, Paris.

Devienne, M., 1958: *Frottements et échanges thermiques dans les gaz raréfiés.* Gauthier-Villars, Paris.

Kirsh, A.A. and *Stechkina, I.B.*, 1978: In *Fundamentals of Aerosol Science* (ed.: *D.T. Shaw*). Wiley Intersci., New York.

Lenoble, J., 1993: Influence des aérosols atmosphériques sur le rayonnement: conséquences climatiques, possibilités de télédétection. *COFERA GAMS*, 75-80.

Manson, D.R., 1984: In *Aerosols: Science, Technology and Industrial Applications.* (eds.: *B.Y.H. Liu, D.Y.H. Pui* and *H.J. Fissan*). Elsevier, New York.

Monson, D.P., 1988: In *Proceedings of 1988 Annual Meeting of AAAR.* Chapel Hill, NC.

Payet, S., 1992: Filtration stationnaire et dynamique des aérosols liquides submicroniques. *Thèse de l'Université Paris XII. Rapport CEA-R-5589.*

Rubow, K.L., 1981: Submicron aerosol filtration characteristics of membrane filters. *Ph.D. Dissertation.* Mechanical Engineering Dept., Univ. of Minnesota, Minneapolis, MN.

Zhang, Z. and *Liu, B.Y.*, 1992: Experimental study of aerosol filtration in the transition flow regime. *Aerosol Science and Technology 15*, 228-238.

APPENDIX 1

Referring to Fig. 3., given in the text, *the derivation of the exponential relationship* given by Eq. (1) is as follows.

Operating in the laminar regime, the pressure difference, $\Delta p(t) = p_1(t) - p_2(t)$, decreases according to the exponential relationship:

$$\Delta p(t) = \Delta p(0) \exp\left[-\frac{t}{\tau}\right]. \tag{1}$$

Indeed, considering air as a perfect gas, we have inside each of the two tanks:

$$p_1 V_1 = \frac{m_1}{M} R T_1,$$

and

$$p_2 V_2 = \frac{m_2}{M} R T_2,$$

where R is the universal gas constant; m_1 is the mass of air in tank I; m_2 is the mass of air in tank II; T_1 and T_2 are the respective absolute temperatures in

tanks I and II; V_1 and V_2 are their respective volumes. The tanks are at the same temperature and have equal volumes.

Subsequently: $T_1 = T_2 = T,\ V_1 = V_2 = V.$

Which gives:

$$p_1 V = \frac{m_1}{M} RT \Rightarrow \frac{RT}{MV} = \frac{p_1}{m_1}, \tag{A1.1}$$

$$p_2 V = \frac{m_2}{M} RT \Rightarrow \frac{RT}{MV} = \frac{p_2}{m_2}. \tag{A1.2}$$

Therefore, for the relationship to be valid at any moment:

$$\frac{p_1}{m_1} = \frac{p_2}{m_2}. \tag{A1.3}$$

Our system (tanks I and II and their connecting pipes) is totally isolated from the 'outside', so that the total mass of air is constant, therefore:

$$\begin{aligned} m_1 + m_2 &= m_0, \\ m_2 &= m_0 - m_1. \end{aligned} \tag{A1.4}$$

Relationship (3) becomes:

$$p_2 = p_1 \left[\frac{m_0}{m_1} - 1 \right]. \tag{A1.5}$$

The total pressure is also constant, so:

$$p_1 + p_2 = \text{constant}. \tag{A1.6}$$

The mass flow, dm, leaving tank I towards tank II during a period of time, dt, is given by the equation:

$$dm = K(p_1 - p_2)\,dt. \tag{A1.7}$$

Where K is the circuit resistance to flow; a real constant in the laminar flow *(Comolet*, 1976).

In this case, tank I loses mass to the benefit of tank II. This means dm_1 is negative, so:

$$dm_1 = -K(p_1 - p_2)\,dt = K(p_2 - p_1)\,dt\,. \tag{A1.8}$$

By differentiating Eq. (1), we get:

$$dm_1 = \frac{VM}{RT}\,dp_1 = K(p_2 - p_1)\,dt\,, \tag{A1.9}$$

subsequently:

$$dm_1 = \frac{VM}{RT}\,dp_1 = K(p_2 - p_1)\,dt\,,$$

and: $$p_1 + p_2 = p_0 \Rightarrow p_2 = p_0 - p_1,$$

thus:

$$\frac{VM}{RT}\,dp_1\,K[(p_2 - p_1) - p_1]\,dt = K[p_0 - 2p_1]\,dt\,,$$

and then:

$$\frac{dp_1}{p_0 - 2p_1} = K\frac{RT}{VM}\,dt\,.$$

Which after integration gives:

$$(p_0 - 2p_1) = C_0^2 \exp\left[-2K\frac{RT}{VM}\,t\right].$$

The integration constant, C_0^2, is determined by the initial conditions for the pressures p_1 and p_2 inside each of the two tanks before their connection, and:

$$p_1(0) \text{ is known at } t = 0,$$
$$p_2(0) \text{ is known at } t = 0,$$

also known at $t = 0$:

$$p_1(0) + p_2(0) = p_0.$$

Then at $t = 0$:

$$p_0(0) - 2p_1(0) = C_0^2 \exp(0),$$

$$C_0^2 = p_0 - 2p_1(0)\,,$$

$$C_0^2 = p_2(0) - p_1(0)\,. \tag{A1.11}$$

Therefore:

$$2p_1(t) = p_0 \{p_2(0) - p_1(0)\} \exp\left[-2\frac{KRT}{VM}t\right],$$

$$p_1(t) = \frac{p_1(0)}{2}\left[1 - \exp\left[1 - 2\frac{KRT}{VM}t\right]\right] + \frac{p_2(0)}{2}\left[1 - \exp\left[-2\frac{KRT}{VM}t\right]\right]. \quad \text{(A1.12)}$$

We have: $p_0 = p_1(t) + p_2(t) = \text{constant},$

so: $p_2(t) = p_0 - p_1(t) = p_1(0) + p_2(0) - p_1(t),$

subsequently: $p_2(t) = p_1(0) + p_2(0) - p_1(t).$ (A1.13)

Replacing $p_1(t)$ by its expression given by Eq. (11) we get:

$$p_2(t) = p_1(0) + p_2(0) -$$

$$\left\{\frac{p_1(0)}{2}\left[1 - \exp\left[-2\frac{KRT}{VM}t\right]\right] + \frac{p_2(0)}{2}\left[1 - \exp\left[-2\frac{KRT}{VM}t\right]\right]\right\},$$

rearranging this equation we get:

$$p_2(t) = \frac{p_1(0)}{2}\left[1 - \exp\left[-2\frac{KRT}{VM}t\right]\right] + \frac{p_2(0)}{2}\left[1 - \exp\left[-2\frac{KRT}{VM}t\right]\right]. \quad \text{(A1.14)}$$

$\Delta p(t)$ is the pressure difference, $[p_2(t) - p_1(t)]$, between the two tanks at any moment:

$$\Delta p(t) = p_1(t) - p_2(t) = [p_1(0) - p_2(0)] \exp\left[-2K\frac{RT}{VM}t\right],$$

$$\Delta p(t) = \Delta p(0) \exp\left[-2\frac{RT}{VM}t\right].$$

Let us consider:

$$\tau = \frac{VM}{2KRT}.$$

Finally, $\Delta p(t)$ becomes:

$$\Delta p(t) = \Delta p(0) \exp\left[-\frac{t}{\tau}\right]. \tag{1}$$

APPENDIX 2 (derivation of Eq. (3))

Determination of the variation in air mass difference between I and II as a function of time ($m_1(t)$ and $m_2(t)$), and of the mass transferred from I to II

$$p_1(t) = m_1 \frac{RT}{MV} \quad \text{in tank I,} \tag{A2.1}$$

$$p_2(t) = m_2 \frac{RT}{MV} \quad \text{in tank II.} \tag{A2.2}$$

$$m_1 + m_2 = \text{constant} \Rightarrow \frac{dm_1}{dt} + \frac{dm_2}{dt} = 0 \Rightarrow \frac{dm_1}{dt} = -\frac{dm_2}{dt}. \tag{A.2.3}$$

Eq. (A2.1) gives:

$$\frac{dp_2}{dt} = \frac{RT}{MV}\frac{dm_2}{dt}. \tag{A2.4}$$

On the other hand, at any moment we have:

$$\frac{dm_1}{dt} = -K(p_1 - p_2).$$

Therefore, by replacing p_1 and p_2 with their values given by Eq. (2) and (A2.1), we get:

$$\frac{dm_1}{dt} = -K\frac{RT}{VM}(m_1 - m_2). \tag{A2.5}$$

From the derivation, Eq. (A2.5) gives:

$$\frac{d^2m_1}{dt^2} = -K\frac{RT}{MV}\left[\frac{dm_1}{dt} - \frac{dm_2}{dt}\right]. \tag{A2.6}$$

Eq. (A2.3) thus leads to:

$$\frac{d^2m_1}{dt^2} = -2K\frac{RT}{MV}\frac{dm_1}{dt}. \tag{A2.7}$$

Considering: $U = \frac{dm_1}{dt}$, Eq. (A2.6) becomes:

$$\frac{dU}{dt} = -2K\frac{RT}{MV}U. \tag{A2.8}$$

After integration, we get:

$$\frac{dm_1}{dt} = U_0 \exp\left[-2K\frac{RT}{VM}t\right].$$

Subsequently:

$$m_1 = -U_0\frac{MV}{2KRT}\exp\left[-2K\frac{RT}{MV}t\right] + A.$$

The integration constants, U_0 and A, are determined by the boundary conditions as follows:

at $t = 0$ $\quad m_1(0) = m_{1,0}$ and $m_2(0) = m_{2,0}$,

as $t \to \infty$ $\quad m_1(\infty) = \frac{m_{1,0} + m_{2,0}}{2} = m_2(\infty)$.

We then get:

$$m_1(t) = \frac{m_{1,0} + m_{2,0}}{2} + \left[\frac{m_{1,0} - m_{2,0}}{2}\right]\exp\left[-2K\frac{RT}{MV}t\right]. \tag{A2.9}$$

A similar calculation gives the evolution of air mass, m_2, in tank II as a function of time:

$$m_2(t) = \frac{m_{1,0} + m_{2,0}}{2} - \left[\frac{m_{1,0} - m_{2,0}}{2}\right]\exp\left[-2K\frac{RT}{MV}t\right]. \tag{A2.10}$$

The difference of mass (i.e., of matter) between I and II is given, at any moment, by:

$$\Delta m(t) = m_1(t) - m_2(t) = \left(m_{1,0} - m_{2,0}\right) \exp\left[-2\frac{KRT}{MV}t\right],$$

$$\Delta m(t) = \Delta m_0 \exp\left[-2\frac{KRT}{MV}t\right],$$

where: $\Delta m_0 = (m_{1,0} - m_{2,0})$.

In the end:

$$\Delta m(t) = \Delta m_0 \exp(-t/\tau), \tag{A2.11}$$

where:

$$\tau = \frac{MV}{2KRT}.$$

We have:

$$m_{1,0} = \frac{VM}{RT} p_{1,0},$$

and:

$$m_{2,0} = \frac{VM}{RT} p_{2,0},$$

where $p_{1,0}$ and $p_{2,0}$ are the pressures in tank I and II, respectively, at $t = 0$. Thus,

$$m = \frac{m_{1,0} - m_{2,0}}{2} = \frac{VM}{RT}\left[\frac{p_{1,0} - p_{2,0}}{2}\right].$$

Therefore:

$$m = \frac{VM}{2RT}\Delta P_0, \tag{3}$$

Δp_0 being the difference of pressures between tanks I and II at $t = 0$.

IDŐJÁRÁS

Quarterly Journal of the Hungarian Meteorological Service
Vol. 98, No. 3, July–September 1994

Ozone episodes in Hungary in March

V. Sándor, L. Haszpra and **Gy. Baranka**

Institute for Atmospheric Physics,
P.O. Box 39, H-1675 Budapest, Hungary

(Manuscript received 28 June 1994; in final form 26 September 1994)

Abstract—Every year there are a few days in March when the daily maximum 30 minutes average ozone mixing ratio exceeds 60 ppbv in Hungary. In this paper the reasons for these early spring ozone episodes are studied. It is found that the majority of the episodes is formed when the weather in the Carpathian Basin is controlled by anticyclones causing dry, sunny weather. However, long range transport of ozone and precursors, local ozone formation (urban plume) and intrusion of free tropospheric air into the surface layer may also result elevated ozone concentration. Meteorological factors characterizing the above processes can be reliably forecasted.

Key-words: ozone, ozone episodes, ozone forecasting, meteorological conditions.

1. Introduction

In the industrialised regions the majority of ozone observed in the surface layer is formed photochemically from ozone precursors like nitrogen oxides, carbon monoxide and reactive organic substances. The rates of the photochemical reactions directly depend on the incoming solar radiation. Therefore, the highest ozone concentrations are measured during the summer season. However, in certain cases rather high concentration can be observed as early in the year as March, while usually after late September elevated concentrations rarely occur. Most of the authors refer to the influence of the stratospheric ozone having its maximum over the northern mid-latitude in spring (*Haagenson et al.*, 1981; *Johnson* and *Viezee*, 1981; *Raatz et al.*, 1985; *Vaughan* and *Price*, 1989; *Ebel et al.*, 1991; *Oberreuter*, 1992; *Gruzdev* and *Sitnov*, 1993). However, this asymmetrical behaviour may also be caused by the interaction of the increasing insolation with the high amount of ozone precursors accumulated in the atmosphere during winter (*Penkett* and *Brice*, 1986—see also

Fig. 1 for Hungary). In this paper the meteorological conditions resulting in elevated ozone concentration in March are studied on the basis of the measurements carried out at K-puszta regional background air pollution monitoring station located in the centre of Hungary (46°58′N, 19°33′E, 125 m masl). Continuous ozone monitoring was started at this side in January, 1990.

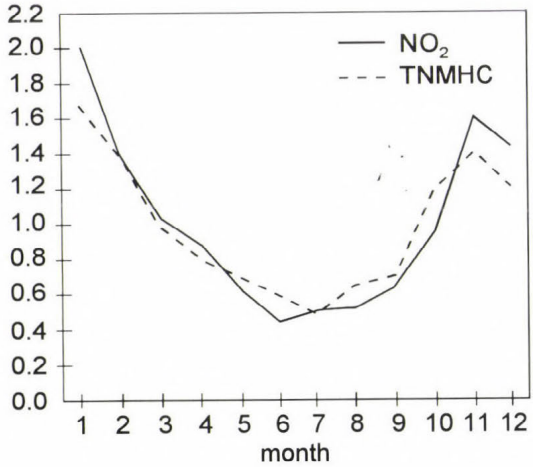

Fig. 1. Average relative (monthly average/annual average) annual cycles of NO_2 and total non-methane hydrocarbon concentrations at K-puszta (1987–1993).

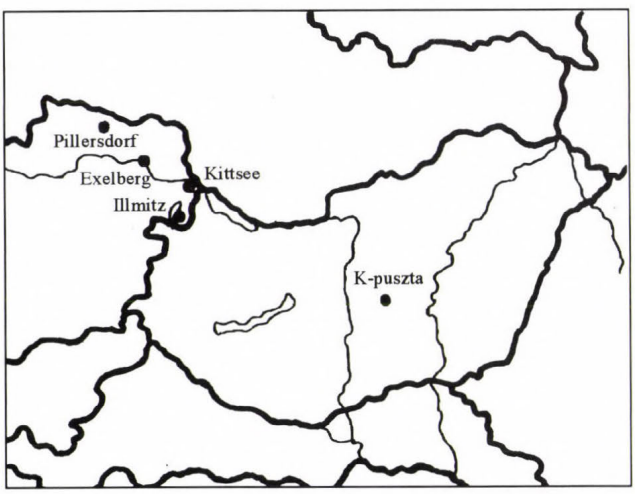

Fig. 2. Ozone monitoring stations in East-Austria and Hungary.

In this study to get a wider scope of the phenomenon measurements at a few ozone monitoring stations in East-Austria were also used (*Fig. 2*).

2. *Ozone episodes in March*

In this paper those days are studied when the maximum 30 minutes average ozone concentration value (mixing ratio) exceeds 60 ppbv for more than one day in succession. Most of these days clusters in 6 episodes (*Table 1*, *Fig. 3*).

Table 1. The periods of the episodes, 1990–1993

Period	O_3 maximum (ppbv)	Day of maximum
15–21 March, 1990	103.7	19 March
15–16 March, 1991	69.5	15 March
21–24 March, 1991	70.2	21 March
5– 7 March, 1993	68.3	6 March
10–17 March, 1993	71.9	16 March
20–23 March, 1993	69.5	22 March

On 21 and 24 March, 1991, the daily maximum 30-minutes ozone concentration exceeded 60 ppbv. However, between these days the measurement was interrupted, therefore, we could not be sure if that period was an episode. In addition to the above episodes there was a day in 1992 (28 March) when the daily maximum ozone concentration exceeded 60 ppbv (61.8 ppbv). The maximum concentration on the preceding day was also high, it reached 55 ppbv. The ozone concentration was governed by different processes on those two days. On the first one the influence of the upper tropospheric (indirectly stratospheric) air might be assumed. Therefore these days are also studied in this paper.

Episode 1: 15–21 March, 1990

March 1990 was drier and warmer than usual. Since 14 March the weather in the Carpathian Basin was influenced by an extended high pressure area (max. 1050 hPa) which had its centre over the Basin on 19 March (*Fig. 4*). The temperature gradually increased up to 9°C above the multiannual average and the sunshine duration was as long as 76–92% of the astronomically potential one. Only weak easterly wind was observed during the period. The meteorological condition was favourable for photochemical oxidant formation and accumulation in the whole region (*Fig. 5*). All monitoring stations in the region measured high concentration due to the similar meteorological conditions, however, the maximum values differed, which might reflect the importance of local effects (concentration of precursor and reductive compounds, dry deposition of ozone, etc.). The accumulation process was interrupted by a weak cold front passing the Carpathian Basin on 21 March.

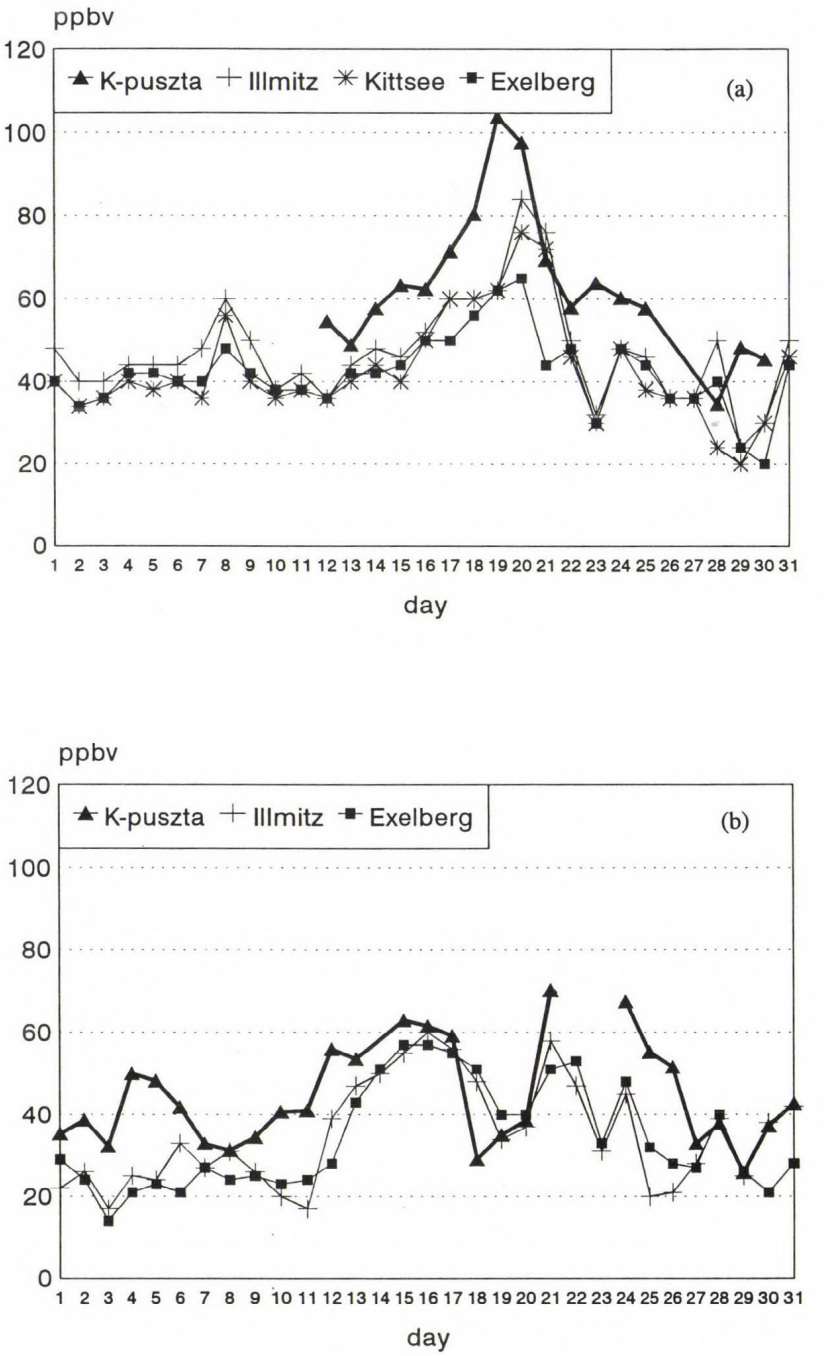

Fig. 3. The daily maximum 30 minutes ozone mixing ratios (*a*) March 1990, (*b*) March 1991.

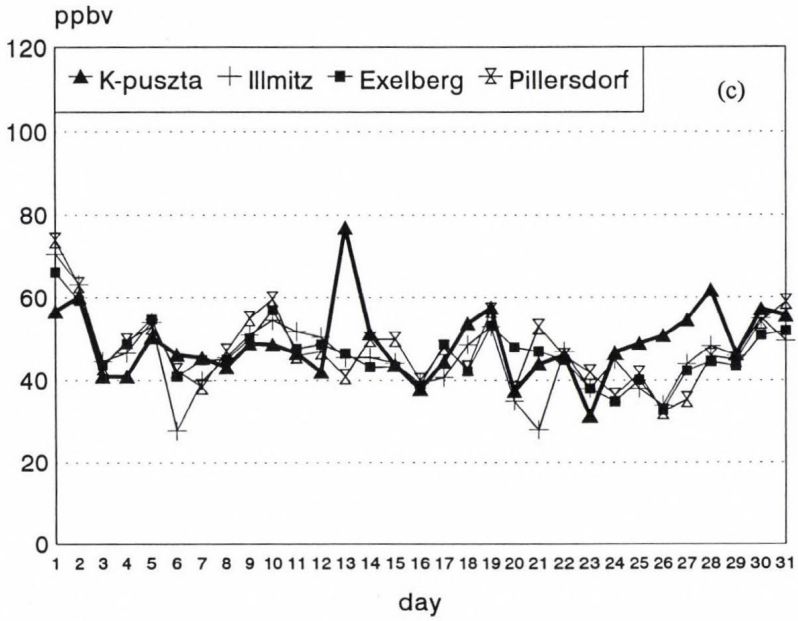

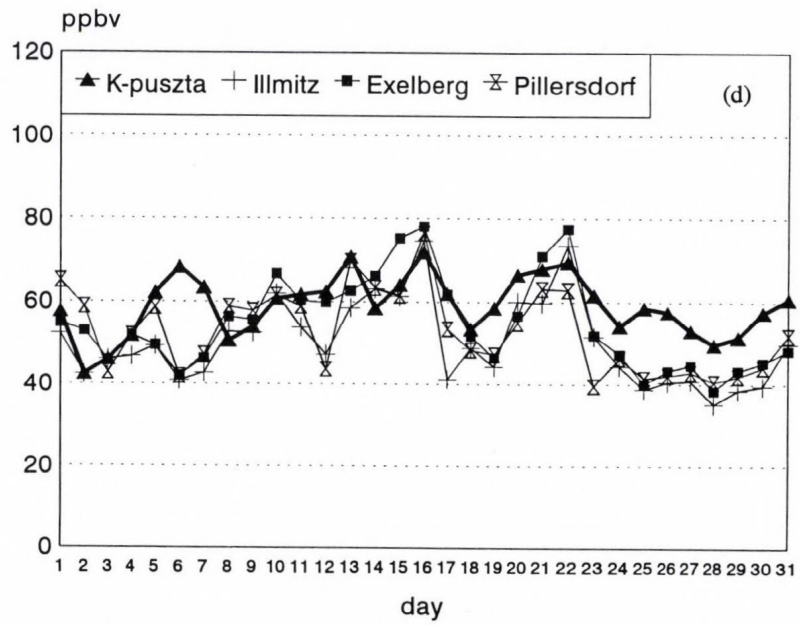

Continuation of *Fig. 3*.....(*c*) March 1992, (*d*) March 1993.

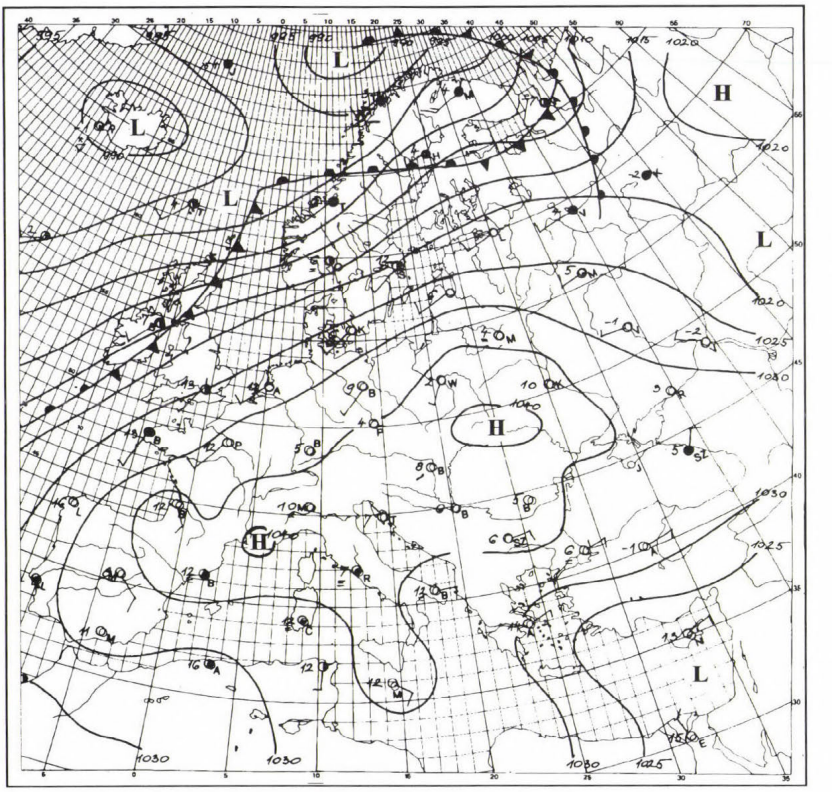

Fig. 4. Synoptic chart for 19 March, 1990, 00 UTC.

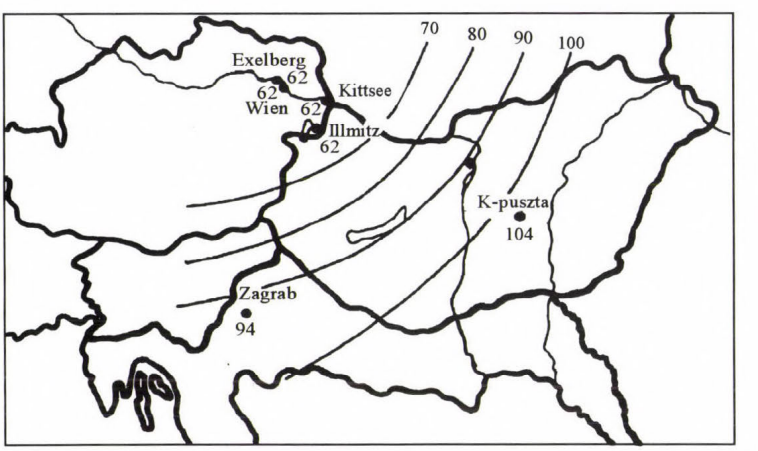

Fig. 5. Spatial distribution of the daily maximum 30 minutes ozone concentration on 19 March, 1990.

Episode 2: 15–16 March, 1991

Between 12 and 16 March a high pressure area controlled the weather in the Carpathian Basin. It resulted in a dry, a bit warmer than usual period. The accumulation of ozone in the surface layer started on 12th, however, the daily maximum concentration exceeded 60 ppbv only on 15 and 16 March. The changeable, rainy weather significantly decreased the ozone concentration after 17 March.

Episode 3: 21–24 March, 1991

Following the influence of a weak anticyclone the weather of the Carpathian Basin was determined by the forward side of a low pressure area having its centre over Western Europe. The resulted weak-to-moderate southwest air flow (later south, southeast) increased the temperature well above the usual. The dry, sunny period favoured the local ozone formation, however, the regional or long-range transport of ozone and its precursors from the sunny Southern Europe might also contribute to the high concentrations. The period was closed by the intrusion of cold air mass on the back side of the low pressure area moving slowly to east.

Episode 4: 27–28 March, 1992

Before the cold front passing over K-puszta at about 7 a.m. local time on 27 March the ozone concentration gradually increased up to 46 ppbv. However, right before the front it fell down 15 ppbv in one and a half hour. Behind the front, in spite of the early time of the day, the concentration quickly increased again and the daily maximum (55 ppbv) was reached before noon (*Fig. 6*).

The isentropic trajectory reaching K-puszta in the morning on 27 March (*Fig. 7*) reflects a remarkable transport of air from the upper troposphere (5–6000 m) to the lower layer from which it could be mixed into the surface layer. As the ozone concentration in the free troposphere increases with height (*Brühl* and *Crutzen*, 1989; *WMO*, 1990), this vertical transport might mix ozone rich air close to the ground causing the sudden increase of the ozone concentration observed.

The sunny weather on the next day promoted the local ozone formation.

Episode 5: 5–7 March, 1993

March 1993 was dry but cooler and less sunny than usual. The period of 5–7 March, which was not favourable for ozone formation in general, was characterized by moderate northerly wind. Elevated ozone concentration was observed only at K-puszta which reflects a local phenomenon. During the pe-

riod the station was covered by the plume of Budapest in which the chemical reactions might produce high amount of ozone in spite of the unfavourable photochemical condition. By means of mathematical models further studies are in progress for the determination of the essential meteorological conditions required by the significant ozone formation in the urban plume.

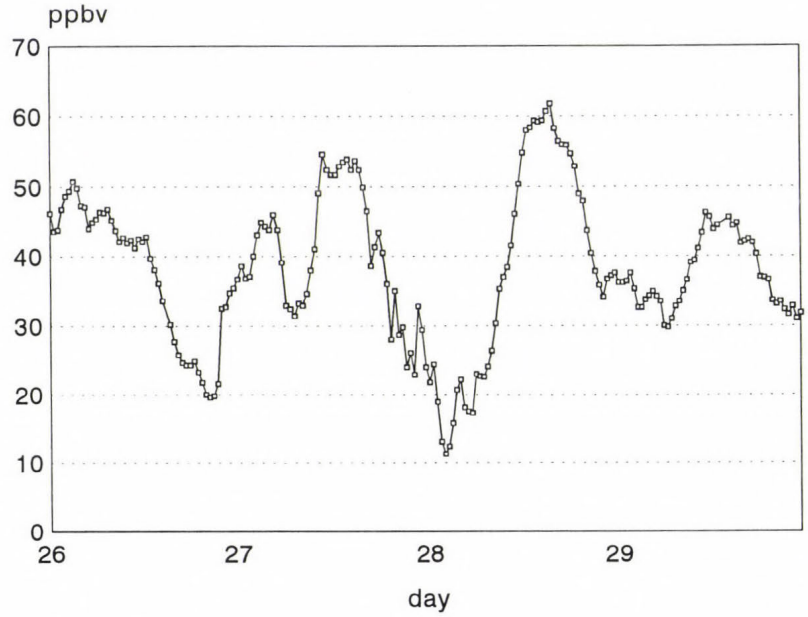

Fig. 6. Diurnal variation of ozone concentration at K-puszta, 26–29 March, 1992.

Episode 6: 10–17 March, 1993

This period was not favourable for ozone formation either. However, except for 14 March, the daily maximum concentration values at K-puszta were above 60 ppbv. The East-Austrian monitoring stations also reported elevated ozone concentrations.

During the period both the horizontal and vertical air motions were weak. The 96 h backward trajectories arrived at K-puszta originated within a region of 300–400 km around the station. Therefore, it is assumed that the regional scale ozone episode observed was the result of an accumulation process in the above region.

Episode 7: 20–23 March, 1993

After a cold front passing the Carpathian Basin on 19 March the weather was controlled by a weak anticyclone. The warm and sunny weather favoured

the oxidant formation. The accumulation process was interrupted by a cold front passing K-puszta in the afternoon on 23 March.

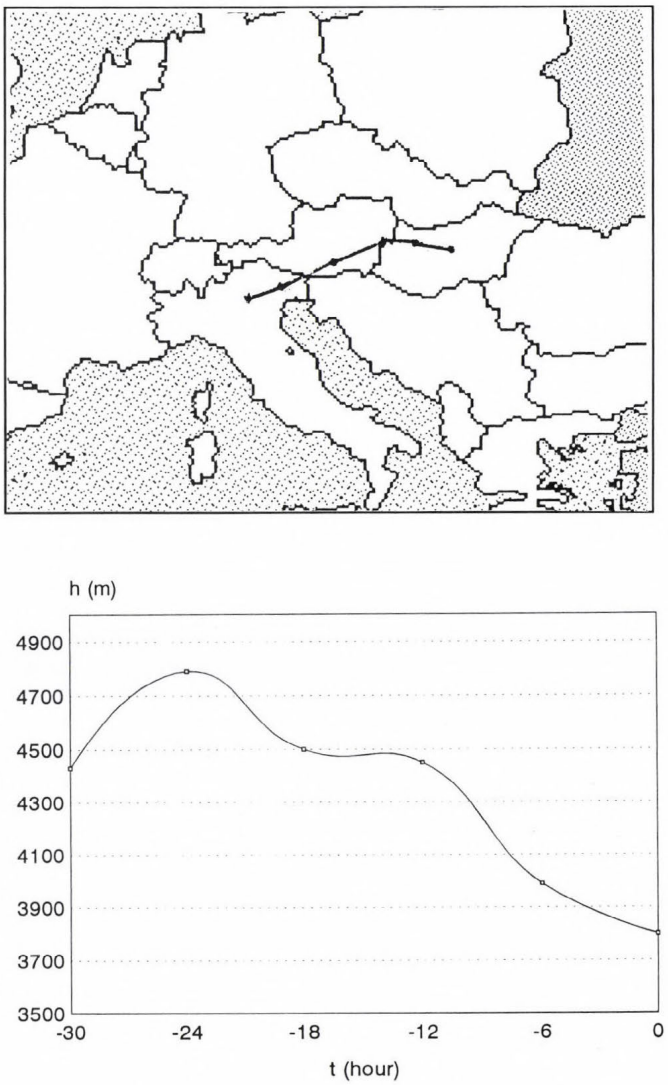

Fig. 7. (*a*) Isentropic trajectory arriving at K-puszta at 12 UTC, 27 March, 1992; (*b*) The height of the above isentropic trajectory.

3. Classification of the episodes

In the majority of the episodes presented here high ozone concentrations were formed when the weather in the Carpathian Basin was controlled by

anticyclones. The dry, sunny, calm weather characterizing these periods resulted in elevated ozone concentrations not only at K-puszta but in an extended region. This was the case in *Episodes 1, 2, 3* and *7*. The second day of *Episode 4* can also be listed here. In these cases the macrosynoptic conditions were the determining factors.

In the rest of the episodes different reasons led to elevated ozone concentration, or the reason could not be identified. On the first day of *Episode 4* the intrusion of upper tropospheric air forced by meteorological fronts can be made responsible for the high concentration. In *Episode 5* the ozone formation in the urban plume of Budapest covering the station may be the explanation for the elevated concentration. The spatially extended *Episode 6* needs further investigation.

Obviously the processes can support each other. For example, during *Episode 4* the downward ozone transport from the free troposphere contributed to the elevated ozone level on the second day when the local formation was also intensive.

Studying the relation between the macrosynoptic condition and the daily maximum ozone concentration we found that high ozone concentrations can be expected if the relative sunshine duration is larger than 60% of the potential one AND the weather is warmer than usual (deviation of the temperature from the multiannual average is positive) AND the pressure gradient remains below 1.0 hPa/100 km. On 60% of days satisfying this condition the daily maximum 30–minutes ozone concentration exceeds 60 ppbv (*Fig. 8*). The highest concentrations may occur when the weather is significantly warmer ($> 6°C$) than usual (multiannual average temperature at K-puszta is 6.5°C), the relative sunshine duration is longer than 70% of the astronomically potential one and the pressure gradient remains below 0.5 hPa/100 km. The meteorological parameters in the above condition can be forecasted reliably. This means that a significant portion of the early spring ozone episodes can also be forecasted with acceptable effectiveness.

The sunny weather alone is not enough for the formation of elevated ozone concentration. If the temperature anomaly is negative the daily maximum concentration rarely exceeds 60 ppbv (*Fig. 9*).

The meteorological conditions leading to high concentration are often satisfied when the weather of the Carpathian Basin is controlled by a high pressure area having its centre over the Basin or to the south of it. Taking into account the average frequency of occurrence of such a meteorological situation, there may be 4–5 days in March when the daily maximum concentration can be expected above 60 ppbv. In addition, every March there may be a few more days when other causes lead to ozone concentration exceeding this level at K-puszta.

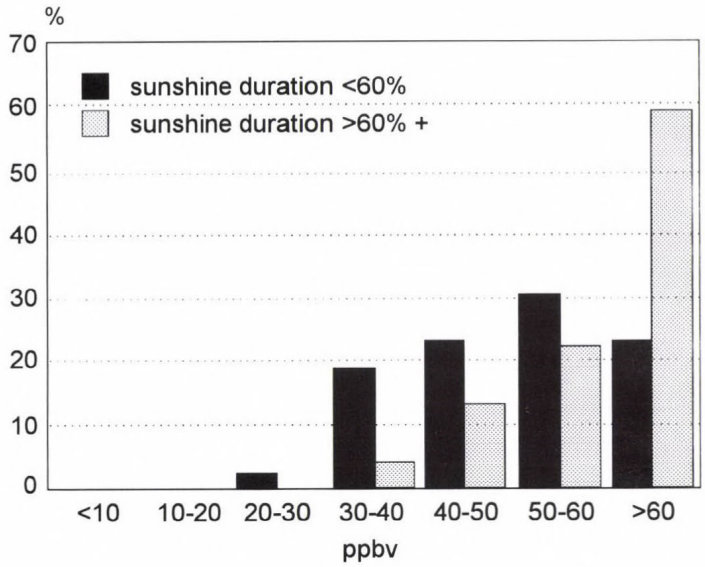

Fig. 8. Relative frequency distribution of the daily maximum 30 minutes average ozone concentration for < 60% relative sunshine duration (all cases) and for > 60% relative sunshine duration with positive temperature anomaly.

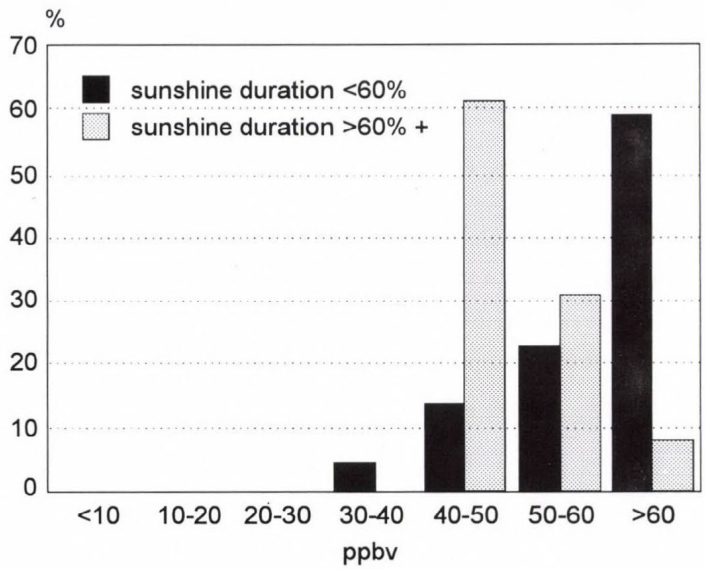

Fig. 9. Relative frequency distribution of the daily maximum 30 minutes average ozone concentration for positive and negative temperature anomaly, if the relative sunshine duration is higher than 60%.

Acknowledgements—The study was sponsored by the National Committee for Technological Development, Budapest, as part of an EUREKA/EUROTRAC/TOR contribution (PHARE ACCORD H9112-0400). The authors highly appreciate the East-Austrian and Croatian ozone data provided by *K. Radunsky* (Umweltbundesamt, Austria) and *L. Klasinc* (Ruđter Bošković Institute, Zagreb, Croatia). The isentropic trajectory was calculated by *I. Ihász* (Inst. for Atmospheric Physics, Budapest).

References

Brühl, C. and *Crutzen, P.*, 1989: On the disproportional role of tropospheric ozone as a filter against UV-B radiation. *Geophys. Res. Letters 16*, 703-706.

Ebel, A., Hass, H., Jakobs, H.J., Laube, M., Memmesheimer, M., Oberreuter, A., Geiss, H. and *Kuo, Y.-H.*, 1991: Simulation of ozone intrusion, caused by a tropopause fold and cut-off low. *Atmos. Environ. 25A*, 2131-2144.

Gruzdev, A.N. and *Sitnov, S.A.*, 1993: Tropospheric ozone annual variation and possible troposphere-stratosphere coupling in the Arctic and Antarctic as derived from ozone soundings at Resolute and Amundsen-Scott stations. *Tellus 45B*, 89-98.

Haageson, P.L., Shapiro, M.A. and *Middleton, P.*, 1981: A case study relating high ground level ozone to enhanced photochemistry and isentropic transport from the stratosphere. *J. Geophys. Res. 86*, 5231-5237.

Johnson, W.B. and *Viezee, W.*, 1981: Stratospheric ozone in the lower troposphere–I. Interpretation of aircraft measurements. *Atmos. Environ. 15*, 1309-1323.

Oberreuter, A., 1992: *Intrusion stratosphärischen Ozons in die Troposphäre durch Tropopausenfaltungen und Kaltlufttropfen.* Mitteilungen aus dem Institut für Geophysik und Meteorologie der Universität zu Köln, Köln.

Penkett, S.A. and *Brice, K.A.*, 1986: The spring maximum in photo-oxidants in the Northern Hemisphere troposphere. *Nature 319*, 655-657.

Raatz, W.E., Schnell, R.C., Shapiro, M.A., Oltmans, S.J. and *Bodhaine, B.A.*, 1985: Intrusions of stratospheric air into Alaska's troposphere, March 1983. *Atmos. Environ. 19*, 2153-2158.

Vaughan, G. and *Price, J.D.*, 1989: Ozone transport into the troposphere in a cut-off low event. Ozone in the Atmosphere. In *Proceedings of the Quadrennial Ozone Symposium 1988 and Tropospheric Ozone Workshop* (eds.: *R.D. Bojkov* and *P. Fabian*). A. Deepak, Hampton, Va., pp. 415-418.

WMO, 1990: WMO consultation on Brewer Ozone Spectrophotometer operation. Calibration and data reporting. *Global Atmosphere Watch, WMO Global Ozone Research and Monitoring Project*, No. 22.

IDŐJÁRÁS

Quarterly Journal of the Hungarian Meteorological Service
Vol. 98, No. 3, July–September 1994

Dry deposition of trace metals in Serbia: a contribution to the methodology of measurement

J. M. Marendić-Miljković, S. F. Rajšić and Z. B. Vukmirović

Institute of Physics,
Pregrevica 118, 11080 Belgrade-Zemun, Yugoslavia

(Manuscript received 22 June 1994; in final form 20 September 1994)

Abstract—An automatic wet/dry precipitation collector for trace metal deposition monitoring in rural and remote areas is constructed in the Institute of Physics, Belgrade. The aim is to simulate dry deposition to natural surfaces in order to estimate the impact of the atmospheric deposition on plants, mainly forests and crops. Dry deposition collector includes polyethylene holder, with two polycarbonate Petri dishes fixed upward and one downward-facing. This design allows both downward and upward fluxes to be measured. A timer for recording the dry period duration is also built in.

The dry deposition collector was tested in clean air of the Kopaonik mountain, Serbia, in two 5-day episodes (June and November 1991), and in Belgrade (November 1992 through October 1993). In the experiment at Kopaonik (site height 1225 m, 40 km downwind from the source), 24-hour mean fluxes were in the range of $\leq$0.02-2.44 ng m^{-2} s^{-1} for Pb, $\leq$0.02–3.5 ng m^{-2} s^{-1} for Cu, and $\leq$0.02–5.19 ng m^{-2} s^{-1} for Zn. Fluxes were very inhomogeneous: C_v (coefficient of variation of the mean) was 0.4–1.2. Ratio of the upward to downward flux, F_R was in the wide range from 0.01 to 16, more than 40% of values being $\geq$1.0. At a suburban Belgrade site, 7-day mean fluxes were measured. Average (n=38) downward fluxes were 0.40 (0.20) ng m^{-2} s^{-1} for Pb, 0.19 (0.14) for Cu, and 0.36 (0.23) ng m^{-2} s^{-1} for Zn (standard deviation in parenthesis). Fluxes were homogeneous, $\bar{C}_v$ was 0.10–0.14. $\bar{F}_R$ is found to be 0.18–0.22.

With a new-designed dry deposition collector an improvement in correspondence between dry deposition sampling and atmospheric processes is achieved.

Key-words: atmospheric deposition, dry deposition, trace metals, heavy metals, precipitation collector.

1. Introduction

It seems that dry deposition of atmospheric pollutants has lost its importance as an air quality indicator. It is not unusual that wet/dry precipitation collectors are used as wet-only collectors in routine measurements. However, measuring

dry deposition of species whose fluxes are dominated by large particles may be best conducted by assessing deposited material rather than focusing on airborne concentrations (*Davidson et al.*, 1985a; *Holsen* and *Noll*, 1992).

Although the number concentration of aerosol particles in the atmosphere is controlled by fine particles, total mass dry deposition may be dominated by sedimentation of the small fraction of coarse airborne particles. Such examples have already been documented for sulfur-containing particles (*Davidson et al.*, 1985a), as well as for Pb (*Davidson* and *Friedlander*, 1978; *Lin et al.*, 1993) and other trace metal-containing particles (*Lindberg* and *Harriss*, 1981; *Davidson et al.*, 1982).

Dry deposition measurements of trace metals are of special interest for investigation of the impact on the biosphere. For instance, deposition appears to be of particular importance in the biogeochemical cycle of Pb; nearly 100% of the estimated total growing-season flux to the forest floor can be accounted for in terms of the atmospheric deposition to the canopy alone. Besides, the estimated ratio of wet to dry deposition of Pb to the canopy during the growing season being 0.8 (*Lindberg et al.*, 1982) suggests a comparable contribution by each process. However, dry deposition of phytotoxic metals, like Pb, can be more harmful for plants than wet deposition. The reasons are longer exposition and interactions between moisture on vegetation and previously dry deposited material that can result in dissolved metal concentrations at the leaf surface which are significantly higher than those in rain alone (*Lindberg et al.*, 1982). Dry deposition measurements of trace metals can also play an important role in agriculture, in the high quality food production.

Wet/dry bucket samplers have been widely criticized (*Hicks*, 1986). Bucket samplers provide accurate measures of the dry deposition of rapidly falling particles. Questions arise regarding the performance of surrogate-surface devices used to measure deposition of small particles influenced by turbulence. An upward facing collection surface mounted above the natural surface might well collect particles carried by downdrafts, but not those carried by updrafts (*Hicks*, 1986). It has been documented that artificial collectors tend to overcollect coarse and undercollect fine particles, compared to the natural objects (*Ibrahim et al.*, 1983; *Lindberg* and *Lovett*, 1985). Efficiency of collecting coarse particles rises with the height of the vessel sides.

Considering the facts above, the need for a new designed wet/dry collector for trace metal monitoring has been imposed upon. An automatic wet/dry deposition sampler is designed in the Institute of Physics, Belgrade, to be used for trace metal deposition monitoring in rural and remote areas. Our work relies on the previous investigations of *Lindberg* and *Harriss* (1981), *Lindberg et al.* (1982), *Lindberg* and *Lovett* (1985), who also used two upward-facing polycarbonate Petri dishes in an automatic sampler of a different design. On the other hand, our experiment is related to the results of *Noll* and *Fang* (1989), *Noll et al.* (1990), who proposed a model for dry deposition of coarse particles

based on their measurements in the atmosphere. They used an aerodynamically shaped surface and measured both downward and upward fluxes. On the basis of these experiences, we constructed an original sampler and developed a method, the performances of which we still investigate.

The basic idea is to simulate dry deposition to the natural surface in order to estimate the impact of the atmospheric deposition on plants, mainly forests and crops. The construction is a compromise between an aerodynamically shaped surface and the demand of simplicity and practicability in routine use.

Both top and bottom surfaces of the vegetation leaf are exposed to the dry deposition. Bottom surface has greater aerodynamical roughness than top surface, and is not exposed to the wet deposition washout so, it is possible that deposited particles shall be retained for a longer time. Moreover, the sizes of the particles deposited on the bottom surface can significantly exceed 1 μm. At an urban site, *Noll et al.* (1988) obtained mass median diameter (MMD) of 70 μm for total particles deposited to the lower plate. *Noll* and *Fang* (1989) estimate the maximum of the deposition velocity on the bottom surface for particle sizes of 20–40 μm.

Therefore, one of the aims of this work is to emphasize the significance of the upward deposition flux measurements.

2. Experimental

2.1 Sampling

Wet and dry collectors are mounted at 2 m height (the height is adjustable) on an aluminum pole (*Fig. 1*). This height has been chosen according to the methodology of dry deposition measurement in forest clearings proposed by *Lindberg* and *Turner* (1988).

The dry deposition collector is a surrogate surface sampler with minimized aerodynamic effects of the walls. The surface is a polycarbonate Petri dish of 94-mm inner diameter with a 13-mm rim. This choice offers several advantages: low substrate background for trace elements in deposition; minimized contamination during handling due to the presence of the rim, ease of efficient extraction by using ultrasonic bath; ready availability at low cost. Besides, the small rim precludes dew and fog drip, even small amount of which result in loss of soluble components from rimless surfaces (*Lindberg* and *Lovett,* 1985). The collector consists of an especially designed holder, made of polyethylene, with two Petri dishes fixed upward-facing and one downward-facing.

An electronically operated rain shield is positioned 1 cm above Petri dishes in the closed (rain protected) position. In the open position this rain shield covers wet deposition collector, protecting the sample from dry deposition contamination.

A rain sensor, heated resistance grid, is placed at the top of the pole. Once

the rain shield is set in a closed position, it stays in that position for at least 5 min. This electronically programmed period prevents numerous opening-closing actions at the beginning of the rain events. (Most rain events begin with scattered rain drops; also, after the rain stops there is, very often, a high relative humidity which may give a false signal.)

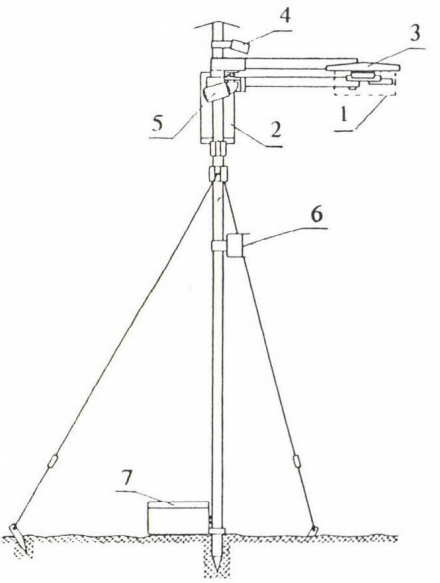

Fig. 1. Automatic wet/dry precipitation collector. (1) dry deposition collector; (2) wet deposition collector; (3) rain shield; (4) rain sensor; (5) motor; (6) control unit; (7) storage battery.

The sensing circuit also controls a timer for recording the dry period duration, expressed in minutes.

The wet deposition collector consists of polyethylene bottle with a funnel, altogether placed in a cylindric housing. A quantitative cellulose filter, fastened in the funnel, filters rainwater removing locally generated wind-blown dust, suspended in raindrops.

In order to minimize the heating and evaporation of the sample, the housing is coated with mirror layer which reflects sunlight. Funnel diameter is related to the minimum sample volume needed for analysis. For a more detailed description see *Marendić-Miljković* and *Vukmirović* (1994).

2.2 *Analytical procedures*

All of the preparatory lab work was conducted in a class 100 clean laboratory. Petri dishes were soaked for 48 hr in dilute nitric acid, and then

thoroughly rinsed with ultrapure water. The purified dishes were wrapped in polyethylene bags and sealed, to be opened just prior to use. All handling of Petri dishes was done using clean polyethylene gloves. After the sampling, dishes were packed back in bags and transported to the clean room.

Particles deposited on Petri dishes were eluted by 10 ml of 0.1 M HNO_3, (pH $\approx$ 1.2) using ultrasonic bath. Nitric acid (Merck suprapure) was diluted with the double distilled, deionized water.

The amount of particulate matter to be collected in a sampling procedure, is determined by the detection limit of the subsequent analytical technique. The analytical technique, chosen according to the aim and the object of the investigation, is one of the most sensitive for heavy metals analysis: electrochemical method named differential pulse anodic stripping voltammetry (DPASV). The instrument used was an EDT anodic stripping voltammeter, model ECP 140, with hanging mercury drop electrode. The samples were analysed for Pb, Cu, Zn and Cd, by the method of standard addition.

An important advantage of DPASV, compared to the other analytical methods, such as atomic absorption spectrometry (AAS), is that it does not contaminate the working place atmosphere with flue gases. With this feature the previously achieved high class clean-air conditions could be maintained.

In ordinary conditions the sensitivity threshold of 0.002 ng m^{-2} s^{-1} in a weekly dry event was reached for the fluxes of metals studied in this work. Consequently, the sensitivity threshold was higher in 24-hour samples for one order of magnitude. It was surprising that Cd flux was under the detection limit in Belgrade weekly samples.

2.3 Site description

The wet/dry precipitation collector made in the Institute of Physics, Belgrade, was tested in clean atmosphere of the Kopaonik mountain in two episodes (June and November 1991), and in Belgrade under the UN sanctions (November 1992 through October 1993).

The Kopaonik mountain, Serbia, (the highest peak Pančićev vrh, 43°16′21″N, 20°49′26″E, 2017 m amsl), is a 80 km long and 40–60 km wide massif, spreading in the NNW-SSE direction (*Fig. 2*). With this space and height Kopaonik is dominating surrounding area. Deep valleys of the rivers Ibar and Z. Morava surround the mountain from the west and north, while several smaller river valleys penetrate the massif laterally. Such complex orography strongly influences the flow of the air masses producing a transversal jet. Concretely, when the air flow on higher altitudes changes its direction from the S to the NW, the wind at Kopaonik will have stable SW direction, orthogonal to the ridge. These facts are connected with the unfavorable conditions of ventilation and transport of air pollutants in the valleys around Kopaonik, and their elevation from the valleys to the bigger heights (*Gburčik*, 1990).

Kopaonik is rich in ore deposition, especially lead and zinc. At the foot of the mountain there is a Lead and Zinc Refinery, with the 312 meters high stack, built in the period of 1982–1984. The stack height is projected to be greater than the inversion height in most weather situations during the whole year. It has been found that a plume from this stack impinges on the south-southwest slopes and the upper regions of Kopaonik (*Tasić* and *Vukmirović*, 1994).

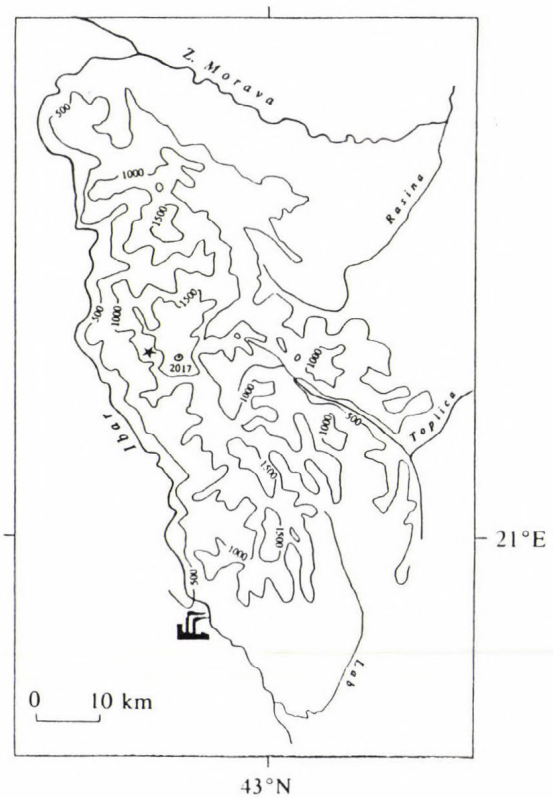

Fig. 2. The Kopaonik mountain. ★ Experimental site Glog (1225 m); ⊙ Pančićev vrh (2017 m); The Lead and Zinc Refinery is indicated as major industrial source.

In our experiment, the site was on the northwest slope of the mountain, at 1225 m amsl height, about 40 km far from the source. It is a location named Glog, in a rural area (500 m distant from little village Lisina). In the vicinity, (100 m), there is a non-asphalt road with very rare traffic. There are no local emission sources. The sampling device was placed above a grassy terrain, height of the grass was about 50 cm in June and 1 cm in November. According to *Sehmel* (1980) the aerodynamic surface roughness, $z_0 \approx 0.15$ h, was 7.5 and 0.15 cm, respectively).

In the Belgrade experiment, the site was in a recreative area of new Belgrade (44°48′N, 20°24′E). Actually, it is a large clearing in the park. It is a flat terrain at the confluence of the Sava and Danube rivers. A flat island lies in the Danube dividing the flow where it meets the Sava. The old city lies on the ridge across the Sava river. The characteristics of the air flow combining orographyc complexity, heat island effects, and changes in surface, are difficult to contemplate. The site may be classified as suburban.

3. Results and discussion

The exposure time of the downward-facing Petri dish is different from this of the upward-facing Petri dishes. While the latter are protected during the rain and fog periods, the former is exposed all the time. So, some contribution of the wet and cloud-water deposition to the total deposition on the downward-facing surface cannot be excluded.

Petri dishes with dry deposition samples were taken every day at 12^h during the episodic measurements at Kopaonik. In the Belgrade experiment Petri dishes were changed after 7 days, also at 12^h. Thus, fluxes measured at Kopaonik are 24-hour mean values, while fluxes measured in Belgrade are 7-day means.

Wind speeds in the June episode were low to moderate (daily averages were 1–4 m s^{-1}) with a stable SSW direction. Friction velocities, according to *Sehmel* (1980), were 20–50 cm s^{-1}. In the November episode the wind speeds were very low (daily av. 0.17–1.20 m s^{-1}), wind direction changed from the SSW to WSW and W. Estimated friction velocities were 2–8 cm s^{-1}.

Dry deposition fluxes obtained in two episodes at the Kopaonik site are presented in *Table 1*. There are several features to be pointed out:

(a) fluxes are generally high for the rural area (maximum value of 2.44 ng m^{-2} s^{-1} of Pb approaches urban levels);

(b) values of fluxes vary over two orders of magnitude, 24-hour mean downward fluxes were in the range of $\leq$0.02–2.44 ng m^{-2} s^{-1} for Pb, $\leq$0.02–3.5 ng m^{-2} s^{-1} for Cu, and $\leq$0.02–5.19 ng m^{-2} s^{-1} for Zn;

(c) there are significant differences between the results on two adjacent upward-facing Petri dishes, in some cases they differ in one (Pb, Cu) and even two (Zn) orders of magnitude. Obviously, fluxes were very inhomogeneous: coefficients of variation of the mean were: 0.4–0.7 for Pb; 0.4–1.1 for Cu and 1.1–1.2 for Zn (in the first episode in June 1991 besides two Petri dishes on the automatic sampler, there were additional four Petri dishes operated manually);

(d) the most interesting feature in *Table 1* is the upward flux: some of these values are extremely high, and even higher than the downward flux values; this needs an explanation.

The upward-facing surfaces generally collect more material than downward-facing ones. It was particularly surprising that in the Kopaonik experiment there

were many exceptions to the rule. In approximately 40% cases downward-facing Petri dish collected equal or more measured metals than the upward-facing dish. A particle deposition flux ratio F_R (defined as the ratio of the upward flux to the downward flux) is expected to be < 1. Values of F_R were in the vide range from 0.01 to 15, about 40% of values being ≥ 1.0. Extreme value obtained was $F_R > 15$ for Pb.

Table 1. Dry deposition fluxes. Episodes of June and November 1991, Kopaonik. The arrows indicate the direction of the flux

Date	Dry deposition flux (ng m^{-2} s^{-1})					
12^h–12^h	↓ Pb	↑	↓ Cu	↑	↓ Zn	↑
1991						
06/18–19	1.22	≤0.02	0.28	0.12	1.06	≤0.02
	2.12		0.25		1.06	
06/19–20	0.90	≤0.02	0.15	0.24	0.74	1.06
	1.22		0.29		0.74	
06/20–21	0.35	≤0.02	0.28	0.13	≤0.02	3.89
	0.23		0.06		1.53	
06/21–22	0.24	0.23	0.09	0.36	0.10	1.30
	0.59		1.81		0.84	
11/19–20	0.68	2.13	1.31	1.84	n.a.	≤0.02
	2.44		0.98		n.a.	
11/20–21	2.38	1.77	0.84	2.69	5.19	0.41
	2.32		2.26		3.84	
11/21–22	0.64	0.70	0.48	1.75	0.43	2.32
	0.64		2.27		n.a.	
11/22–23	0.74	≤0.02	0.73	0.12	0.41	≤0.02
	≤0.02		≤0.02		≤0.02	
11/23–30	0.34	0.02	0.01	0.01	0.0-	≤0.02
	0.63		0.02		80.59	

n.a. – not available
Exposure time: $1300 < t \leq 1440$ min

These characteristics are probably due to the presence of a small number of very large particles. Simultaneously measured concentration by the filtration method with two filters in series, one for coarse (> 2 μm) and an other for fine (0.35–2 μm) particles, confirmed this thesis: coarse fraction contained significantly more metals measured than fine fraction, in all samples, see

Marendić-Miljković et al., (1994). It should also be mentioned that the airborne concentrations were high too: e.g. for Pb they ranged from 27–284 ng m^{-3} (*ibid.*). Knowing that deposition velocities are much higher for coarse particles, it is expected that the mass of dry deposited metals in this experiment will be dominated by coarse particles. Moreover, fly ash coarse particles containing Pb and Zn, collected on filters, were identified by scanning electron microscopy (*Tasić* and *Vukmirović,* 1994).

In the only one 7-day sample (11/23–30 1991) there were no high values of the upward fluxes. It is possible that large particles deposited on the downward-facing Petri dish cannot hold on for a longer period of time.

High and inhomogeneous fluxes obtained at Kopaonik indicate that the sampling site is on the direct impact of a major emission source. The reason for this situation is probably by-passing of the filters, the phenomenon that could only be found in 'the Eastern Europe's Environment' (the concept introduced by *Alcamo,* 1992).

The results obtained at a suburban site in new Belgrade give a rather different image. In *Table 2* flux data of a series of 38 weekly samples, for which the exposure time is precisely determined, are presented. There were only 3 dry periods and 5 periods with unmeasurable (< 0.1 mm) precipitation. The average ratio of dry deposition exposure time to total time was 0.77 (standard deviation 0.17).

In contrast to the results from Kopaonik, in Belgrade:

(a) fluxes were low, average downward fluxes were 0.40 (0.20) ng m^{-2} s^{-1} for Pb, 0.19 (0.14) ng m^{-2} s^{-1} for Cu, and 0.36 (0.23) ng m^{-2} s^{-1} for Zn (standard deviation in parenthesis). It should be noted that in all samples the amount of Cd deposited on Petri dishes was not sufficient for analysis. Cd flux was under the detection limit of 0.02 ng m^{-2} s^{-1} for 1 day exposure time (Kopaonik) and 0.002 ng m^{-2} s^{-1} for 7 days exposure time (New Belgrade). In order to 'catch' Cd, sampling time should be increased. Low level fluxes of Pb in Belgrade are due to drastically reduced traffic and industrial activities. An overall decrease of air pollution has been noticed since UN sanctions have been imposed upon Yugoslavia;

(b) values of fluxes are more uniform, even though obtained over much longer period; fluxes are in the range 0.06–0.880 ng m^{-2} s^{-1} for Pb, 0.091-0.580 ng m^{-2} s^{-1} for Cu, and 0.054–1.068 ng m^{-2} s^{-1} for Zn;

(c) fluxes were homogeneous, flux values before March, 17 are arithmetic means of the results obtained on two Petri dishes. Coefficients of variation of the mean were: $\bar{C}_v = 0.13 \pm 0.21$ for Pb, $\bar{C}_v = 0.14 \pm 0.23$ for Cu, and $\bar{C}_v = 0.10 \pm 0.23$ for Zn (errors were calculated according to the Student's distribution, on 95% confidence level). After March, 17 only one of the two upward-facing Petri dishes was analysed, while the other was left for microscopic analysis.

Table 2. Dry deposition fluxes at the new Belgrade site (ng m^{-2} s^{-1}). The arrows indicate the direction of the flux

Period	↓ Pb	↑	↓ Cu	↑	↓ Zn	↑
1992						
11/20–27	0.621	0.066	0.507	0.032	0.782	0.045
12/02–09	0.188	0.087	0.201	0.038	0.189	0.048
12/09–16	0.204	0.021	0.144	0.011	0.667	n.a.
12/16–23	0.880	0.010	0.177	0.012	1.068	0.024
1993						
01/20–27	0.576	0.017	0.340	0.010	0.306	0.018
1/27–2/4	0.347	0.012	0.162	0.005	0.389	0.014
02/04–10	0.304	0.012	0.185	0.024	0.242	0.012
02/10–17	0.274	0.048	0.182	0.027	0.500	0.036
02/17–24	0.159	0.020	0.580	0.022	0.192	0.025
2/24–3/3	0.376	0.013	0.130	0.011	0.148	0.006
03/03–10	0.442	0.012	0.072	0.004	0.347	0.042
03/10–17*	0.45	≤0.02	0.29	≤0.02	0.34	≤0.02
03/17–24	≥0.76	0.24	0.24	≤0.02	0.25	0.24
03/24–31	0.10	≤0.02	0.06	0.045	0.78	0.06
3/31–4/7	0.74	0.10	0.145	0.025	≥0.84	0.09
04/07–14	0.36	≤0.02	0.39	≤0.02	0.10	≤0.02
04/21–28	0.40	≤0.02	≥0.60	0.03	0.20	0.04
4/28–5/5	0.41	0.12	0.17	0.07	≥0.67	0.03
05/05–12	0.52	0.09	0.19	0.05	0.45	≤0.02
05/12–19	0.12	0.10	0.055	0.04	0.30	0.04
05/19–26	0.06	0.06	0.065	0.03	0.17	0.15
5/26–6/2	0.41	0.17	0.12	0.025	0.48	0.31
06/09–16	≥0.62	0.05	0.13	0.04	0.16	≤0.02
06/23–30	0.149	0.082	0.045	0.022	0.054	0.014
07/07–14	0.245	0.034	0.081	0.012	0.248	0.014
07/14–21	0.158	0.037	0.145	0.027	0.054	0.036
07/21–28	0.138	0.030	0.060	0.025	0.279	0.032
08/04–11	0.238	0.007	0.074	0.005	0.205	0.010
08/11–18	0.311	0.008	0.091	0.007	0.307	0.007
8/25–9/1	0.188	0.005	0.065	0.006	0.263	0.005
09/01–08	0.410	0.031	0.096	0.021	0.367	0.005
09/08–15	0.354	0.021	0.137	0.012	0.072	0.026
09/15–22	0.458	0.013	0.109	0.006	0.231	0.007
09/22–29	0.369	0.014	0.099	0.026	0.104	0.008
9/29–10/6	0.797	0.297	0.379	0.059	0.571	0.049
10/06–13	0.823	0.029	0.398	0.008	0.555	0.020
10/13–20	0.376	0.037	0.139	0.016	0.327	0.032
10/20–27	0.375	0.017	0.081	0.023	0.316	0.023

n.a.– not available; * By this date till June 16 sensitivity came down

(d) in the Belgrade experiment, out of 42 weekly samples only one had equal amount of Pb on both downward and upward-facing surfaces, the other one had more (20%) Zn, and the third had 50% more Cu on the downward-facing surface. Average ratio of the mass collected on the downward-facing to the mass collected on the upward-facing Petri dish was found to be: 0.21 (0.23) for Pb; 0.25 (0.26) for Cu, and 0.21 (0.26) for Zn (standard deviation in parenthesis). Flux ratio (n = 38) was in the range 0.01–1.00 for Pb, 0.03–0.49 for Cu, and 0.02–0.88 for Zn. Only 8% of F_R values for Pb and Zn were greater than 0.5. In order to calculate mean flux ratio, only those samples with the ratio of dry to total time $\geq$ 0.75, (n = 23) have been taken into account. $\bar{F}_R$ is found to be 0.22 $\pm$ 0.54 for Pb, 0.18 $\pm$ 0.27 for Cu, and 0.20 $\pm$ 0.47 for Zn (errors were calculated according to the Student's distribution, on 95% confidence level).

Because of the boundary layer structure complexity in this location beside the river, it is difficult to comment the Table 2 in the light of meteorological conditions.

Let us again consider the paradox that Pb fluxes were higher in a rural than in an urban area. A short review of trace metal dry deposition fluxes, obtained on surrogate surfaces, is given in *Table 3*. Out of many various surfaces, only flat and Petri dishes are considered. It seems that fluxes obtained at Kopaonik are among the highest rural values in Table 3. Our results, compared to the results of other authors are closest to the results of *Lindberg et al.* (1982) and *Lindberg* and *Turner* (1988), obtained on a rural type site, exposed to acid precipitations. One should bear in mind that deposition rate on Petri dish is normally greater than on a flat surface, and that teflon flat surface would yield the smallest values (see e.g. *Davidson et al.*, 1985b). On the other hand, shortening of the exposure time from seven to only one day may also result in the higher flux values (see e.g. *Noll et al.* 1990). Nevertheless, the main cause for the extremely high flux values is the high level of the air pollution originating from smelter facilities.

There are not too many direct measurements of dry deposition trace metal fluxes reported in the literature. It is common that these fluxes are estimated from the measured airborne concentrations and modeled deposition velocities (*Lin et al.*, 1993; *Bozó et al.*, 1992; *van Daalen*, 1991; *Dulac et al.*, 1989). Various models for predicting dry deposition velocities (*Sehmel* and *Hodgson*, 1978; *Slinn* and *Slinn*, 1980; *Noll* and *Fang*, 1989) as their inputs include wind speed, atmospheric stability, surface aerodynamic roughness, particle density and particle size distribution. Such procedure is much more reliable when particle size distribution is measured too. Difficulties arise in measuring particles over 10 μm diameter which may have substantial influence on dry deposition mass (*Holsen* and *Noll*, 1992). Incomplete information about complete size distribution of atmospheric particles has a much larger influence on the prediction of flux than the use of different models to predict deposition

velocities *(ibid.)*. Models which use only fine particles concentration (even for Pb in rural areas), and MMD deposition velocity to calculate flux rate, severely underestimate the measured flux *(ibid.)*.

Table 3. Trace metal dry deposition fluxes obtained on surrogate surfaces – a review

Flux (ng m^{-2} s^{-1})	Exp (d)	Surface	Site	Reference
Pb				
<2.3			rural	*Schroeder et al.*, '87
0.13–<6			urban	(review)
0.04–0.17	4–7	polyethylene-flat	rural	*Lindberg & Harriss*, '81
2.0–10	4–11	polyethylene–Petri	rural	*Lindberg et al.*, '82
0.28		leaf		
0.0008–0.0049	7	teflon-flat	remote	*Davidson et al.*, '85b
0.028–0.047	7&14	polycarbonate–Petri	rural	*Lindberg & Turner*, '88
2.7	1	mylar-flat	urban	*Noll et al.*, '90
	5			
<0.02–2.44	1	polycarbonate–Petri	rural	this work
0.06–0.88	7		urban	
Cu				
0.38			urban	*Schroeder et al.*, '87 (review)
0.0054–0.036	7	teflon-flat	remote	*Davidson et al.*, '85b
2.0	1	mylar-flat	urban	*Noll et al.*, '90
1.1	5			
<0.02–3.5	1	polycarbonate-Petri	rural	this work
0.04–0.60	7		urban	
Zn				
<6.4			rural	*Schroeder et al.*, '87
0.17–18.8			urban	(review)
0.009–0.027	4–7	polyethylene-flat	rural	*Lindberg & Harriss*, '81
0.53–1.6	4–11	polyethylene-Petri	rural	*Lindberg et al.*, '82
0.97		leaf		
0.011–0.035	7	teflon-flat	remote	*Davidson et al.*, '85b
0.083–0.10	7&14	polycarbonate–Petri	rural	*Lindberg & Turner*, '88
6.7	1	mylar-flat	urban	*Noll et al.*, '90
4.4	5			
<0.02–5.19	1	polycarbonate–Petri	rural	this work
0.05–1.07	7		urban	

Exp – exposure time in days.

It is interesting to mention that *Bozó et al.* (1992) estimated annual average of dry deposition fluxes, for the former Yugoslavia, as follows: 0.28 ng m^{-2} s^{-1}

for Pb, 0.17 ng m^{-2} s^{-1} for Zn and 0.0073 ng m^{-2} s^{-1} for Cd. All these values are of the same order as the correspondig average values in Table 2 (i.e. 0.40 ng m^{-2} s^{-1} for Pb, 0.36 ng m^{-2} s^{-1} for Zn and $\leq 0.002 - \leq 0.02$ ng m^{-2} s^{-1} for Cd).

There are few data, obtained on surrogate surfaces in the field, concerning upward to downward flux ratio. *Dash* (1983) obtained the ratio of the downward to upward-facing results varying from about 0.2–0.5. *Holsen* and *Noll* (1992) obtained a relatively constant flux ratio of 0.3 in a suburban area of Chicago. These results agree fairly well with our results from the site in new Belgrade.

According to the dry deposition model for atmospheric coarse particles proposed by *Noll* and *Fang* (1989), flux ratio F_R is indicative for the sizes of deposited particles. When F_R is greater than 0.1 it is likely that dry deposition mass is dominated by particles having aerodynamic diameter greater than 5 μm. Another indication for coarse particles could be great dissipation of deposition flux values. Highly inhomogeneous flux may be caused by small number of very large particles.

Coe and *Lindberg* (1987) obtained mass median diameter (MMD) for total particles deposited on leaves about 10 μm; fly ash particles (NMD 2.6–3.4) having MMD of the range 5.6–11 μm. Such particles, deposited on leaves by dry deposition mechanism, are potentially harmful for plants. Especially when dissolved in contact with high acidic fog or cloud droplets. This is particularly important for forests growing above the average cloud-base height.

Plants have not developed their self-protecting system for coarse particles, like human beings and animals. So, we cannot exclude coarse particles from dry deposition monitoring, if we are interested in the trace metals impact on the biosphere.

4. Conclusions

A new designed dry (and wet) precipitation collector with Petri dishes, seems to be an improvement compared to the previous bucket-like design. It is recognized that bucket-like samplers overcollect coarse and undercollect fine particles *(Ibrahim et al. 1983)*. Trapping of coarse particles in the bucket sampler is mainly avoided by using Petri dishes with low rim. The downward-facing Petri dish yield information of the upward flux, which involves small particles influenced by turbulence. In that sense a better correspondence between dry deposition sampling and atmospheric processes is accomplished.

Two adjacent upward-facing Petri dishes give possibility of estimating the homogeneity of the flux and better accuracy of the results.

The upward flux is found to be about 20% of downward flux of Pb, Cu and Zn, for 7-day averaging time in a fairly clean air of Belgrade suburban area.

At the site on the slope of the Kopaonik mountain, which is under the impact of a Lead and Zinc Refinery, and with shorter averaging time of only one day, upward flux varied from $\leq$ 0.01 to 15.9 times downward flux. There is not enough data to estimate the mean flux ratio, but it is indicative that upward flux was greater than downward in 40% of all cases. There are two probable causes for this feature: high inhomogeneity of the flux and short averaging time. At this point, question arises regarding proper averaging time related to the dose and the receptor answer.

It is not a simple task to combine the data obtained in order to estimate the net flux to the underlying surface. Workers familiar with turbulent exchange might rely on the difference between upward and downward fluxes; it is likely that this is appropriate for smooth surfaces, like water surface. However, when the surface in question is deciduous forest in vegetational period, it may be more appropriate to take the sum of the two fluxes.

References

Alcamo, J., 1992: *Coping with Crisis in Eastern Europe's Environment.* Parthenon Publ. Group, New York.

Bozó, L., Alcamo, J., Bartnicki, J. and *Olendrzynski,K.*, 1992: Total deposition budgets of heavy metals over Eastern Europe. *Időjárás 96*, 61-80.

Coe, J.M. and *Lindberg, S.E.*, 1987: The morphology and size distribution of atmospheric particles deposited on foliage and inert surfaces. *JAPCA 37*, 237-243.

Daalen, J. van, 1991: Air quality and deposition of trace elements in the province of South-Holland. *Atmos. Environ. 25A*, 691-698.

Dash, J. M., 1983: *Precipitation Scavenging, Dry Deposition, and Resuspension.* Elsevier Press, New York, p. 883.

Davidson, C.I. and *Friedlander, S.K.*, 1978: A filtration model for aerosol dry deposition: Application to trace metal deposition from the atmosphere. *J. Geophys. Res. 83*, 2343-2352.

Davidson, C.I., Miller, J.M. and *Pleskow, M.A.*, 1982: The influence of surface structure on predicted particle dry deposition to natural grass canopies. *Water Air Soil Pollut. 18*, 25-43.

Davidson, C.I., Lindberg, S.E., Schmidt, J.A, Cartwright, L.G. and *Landis, L.R.*, 1985a: Dry deposition of sulfate onto surrogate surfaces. *J. Geophys. Res. 90(D1)*, 2123-2130.

Davidson, C.I., Goold, W.D., Mathison, T.P., Wiersma, G.B., Brown, K.W. and *Relly, M.T.*, 1985b: Airborne trace elements in Great Smoky Mountains, Olympic, and Glacier National Parks. *Environ. Sci. Technol. 19*, 27-35.

Dulac, F., Buat-Menard, P., Ezat, U., Melki, S. and *Bergametti, G.*, 1989: Atmospheric input of trace metals to the Western Mediterranean: uncertainties in modelling dry deposition from cascade impactor data. *Tellus 41B*, 362-378.

Gburčik, P., 1990: Air circulations over Kopaonik and its surroundings. *Proc. Nature of Kopaonik—Protection and Exploatation. Simp.*, Kopaonik, 19-21 April 1990, Fortuna, Beograd (in Serbian), 113-118.

Hicks, B.B., 1986: Measuring dry deposition: a re-assessment of the state of the art. *Water Air Soil Pollut. 30*, 75-90.

Holsen, T.M. and *Noll, K.E.*, 1992: Dry deposition of atmospheric particles: application ambient data. *Environ. Sci. Technol. 26*, 1807-1813.

Ibrahim, M., Barrie, L.A. and *Fanaki, F.* 1983: An experimental and theoretical investigation of the dry deposition of

particles to snow, pine trees and artificial collectors. *Atmos. Environ. 17,* 781-788.

Lin, J.-M., Fang, G.-C., Holsen, T.M. and *Noll, K.E.*, 1993: A comparison of dry deposition modeled from size distribution data and measured with a smooth surface for total particle mass, lead and calcium in Chicago. *Atmos. Environ. 27A,* 1131-1138.

Lindberg, S.E. and *Harriss, R.C.*, 1981: The role of atmospheric deposition in a deciduous forest. *Water Air Soil Pollut. 16,* 13-31.

Lindberg, S.E., Harriss, R.C. and *Turner, R.R.*, 1982: Atmospheric deposition of metals to forest vegetation. *Science 215,* 1609-1611.

Lindberg, S.E. and *Lovett, G.M.*, 1985: Field measurement of particle dry deposition rates to foliage and inert surfaces in a forest canopy. *Environ. Sci. Technol. 19,* 238-244.

Lindberg, S.E. and *Turner, R.R.*, 1988: Factors influencing atmospheric deposition, stream export, and landscape accumulation of trace metals in forested watersheds. *Water, Air and Soil Pollut. 39,* 123-156.

Marendić-Miljković, J. and *Vukmirović, Z.*, 1994: A newly designed automatic wet/-dry precipitation collector. 2nd International Symposium on Environmental Contamination in Central and Eastern Europe. Budapest, September 20-23, 1994 (accepted).

Marendić-Miljković, J., Rajšić, S. and *Vukmirović, Z.*, 1994: Calibration of the dry part of wet/dry collector in clean air. 2nd International Symposium on Environmental Contamination in Central and Eastern Europe, Budapest, September 20-23, 1994 (accepted).

Noll, K.E., Fang, K.Y.P. and *Watkins, L.A.*, 1988: Characterization of the deposition of particles from the atmosphere to a flat plate. *Atmos. Environ. 22,* 1461-1468.

Noll, K.E. and *Fang, K.Y.P.*, 1989: Development of a dry deposition model for atmospheric coarse particles. *Atmos. Environ. 23,* 585-594.

Noll, K.E., Yuen, P.F. and *Fang, K.Y.P.*, 1990: Atmospheric coarse particulate concentrations and dry deposition fluxes for ten metals in two urban environments. *Atmos. Environ. 24A,* 903-908.

Schroeder, W.H., Dobson, M., Kane, D.M. and *Johnson, N.D.*, 1987: Toxic trace elements associated with airbone particulate matter: a review. *JAPCA 37,* 1267-1285.

Sehmel, G.A. and *Hodgson, W.H.*, 1978: A model for predicting dry deposition of particles and gases to environmental surfaces. DOE Report PNL-SA-6721, Pacific Northwest Laboratory, Richland, WA.

Sehmel, G.A., 1980: Particle and gas dry deposition: a review. *Atmos. Environ. 14,* 983-1011.

Slinn, S.A. and *Slinn, W.G.N.*, 1980: Predictions for particle deposition to natural waters. *Atmos. Environ. 14,* 1013-1016.

Tasić, M. and *Vukmirović, Z.* 1994: Identification of particles emitted from a 312 meters high stack of the Lead and Zinc Refinery in Trepča. 2nd International Symposium on Environmental Contamination in Central and Eastern Europe. Budapest, September 20-23, 1994 (accepted).

IDŐJÁRÁS

Quarterly Journal of the Hungarian Meteorological Service
Vol. 98, No. 3, July–September 1994

Temporal variation of the daily extreme high precipitation in Hungary

I. Schirok-Kriston

Hungarian Meteorological Service,
P.O. Box 38, H-1525 Budapest, Hungary

(Manuscript received 5 April 1994; in final form 25 June 1994)

Abstract—This study presents an examination of the daily precipitation amounts above 30 mm during the 20th century. The basic data used consist of the 90 years (1901–1990) daily precipitation data separated into three periods of 30 years from 6 stations in Hungary. Furthermore, the daily precipitation amounts from all the raingauge network of Hungary (about 800 stations) for the period of 1961–1990 were examined as well. It can be said that the occurrence of the daily high and extreme high precipitation in Hungary during the 20th century does not show a decrease or an increase which would exceed the natural climate variability. A further examination is directed to the annual variation of the daily high precipitation. We can conclude that there is a change in timing of maximum of the frequency occurrence of the daily extreme high precipitation from early summer to the second half of summer. This change of annual variation can be related to the appearance of the seasonal change.

Key-words: climate variability and change, daily precipitation, extreme precipitation, Hungary.

1. Introduction

The global climate change has come worldwide into the limelight of interest of the specialists; and the possibility and the rate of its existence has been studied in a lot of climate models. Some large-scale climate anomalies with severe consequences and the observed changes in concentrations of some atmospheric trace gases have led to intense research in the recent 25 years. These studies include the investigation of reasons of the changes, the interactive processes within the climatic system and the climatic impacts, respectively. The results of the studies about the climate change and its possible regional consequences have been summarized in two volume of 'Climate Variability and Change' edited by *Faragó et al.* (1990, 1991).

On the one hand, these publications give a brief review of the international research activities on variability and change of climate, on the other hand, they give an account on the beginning of the research in Hungary and the first results: 'Using regional estimates for this region derived from large-scale climate scenarios by empirical-statistical methods (that is, a moderate warming of about 0.5°C in annual means which corresponds to the 'low' scenario), the preliminary estimations were concluded as follows: an increase in sunshine-duration by about 10%, decrease of annual precipitation amounts by 10–15%, reduction of frost frequencies in autumn and spring' (*Faragó et al.*, 1990). This change qualitatively corresponds to the simultaneous change in the circulation patterns (i.e., the circulation is expected to become more anticyclonic).

Besides the change of the average values (*Mika*, 1991, 1993), a big importance must be devoted to change of frequencies of the extreme meteorological events (*Schirok-Kriston*, 1983). The extreme meteorological events are risk factors, and the changes of their frequencies must be taken into account either during a durable climate variability or during a climate change. These changes can be the consequences and the indicators of the global change.

A question arises, whether any change of extreme meteorological events, the daily extreme high precipitation amounts, ensue as a result of the global climate change.

2. Data and area for the study

This study presents an examination of the daily precipitation above 30 mm during the 20th century. We use the term *high precipitation*, when the daily rainfall is above 30 mm; and the term *extreme high precipitation* when it is above 70 mm.

The basic data used in this study consist of the 90 years (1901–1990) daily precipitation data from six stations of Hungary (*Table 1*). A long series of stored and controlled daily precipitation data is available only for six stations in the climate data base of the Hungarian Meteorological Service. In our further examination the daily precipitation amounts from about 800 stations were used for the shorter period of 1961–1990.

3. Occurrence of daily high precipitation

Table 1 shows the absolute frequencies of the daily high precipitation above 30, 40, 50, 70 and 80 mm, which were recorded by six stations between 1901–1990. The numbers of the last two column including the daily high precipitation of 30 and 40 mm are related to the regional climatological distribution of the precipitation: the precipitation of 30 and 40 mm in Sopron (West–Hungary)

Table 1. The absolute frequencies of the daily high and extreme high precipitation above 30, 40, 50, 70 and 80 mm in Hungary between 1901–1990

Station	≥ 80	≥ 70	≥ 50	≥ 40	≥ 30
Sopron	2	6	32	87	205
Budapest	1	4	15	41	138
Pécs	1	4	22	50	147
Szeged	–	–	10	34	110
Debrecen	1	2	18	43	103
Miskolc	2	2	27	56	151
Σ	7	18	124	311	854

occurs twice more than in Debrecen representing the Great Hungarian Plain, poorly supplied with rain. This regional difference disappears in case of the daily high and extreme high precipitation above 50 mm.

Since our aim is to examine, whether any change of the frequent occurrence of the daily high precipitation in Hungary during the 20th century exists or not, it is reasonable to separate the data of Table 1 during 1901–1990 into three periods of 30 years. *Table 2* shows the absolute frequency of the daily high and extreme high precipitation above 30, 40, 50, 70 and 80 mm recorded by six stations between 1901–1930, 1931–1960 and 1961–1990, respectively. The numbers (percentages) in the last line of Table 2 show all the observations of six stations during 1901–1990, which are distributed into the three periods of 30 years. The percentage is insignificant when the occurrence of the daily extreme high precipitation is very low. Therefore the first and second coloums of the last line are empty within the three periods. Furthermore, it can be seen that 30–36 percent of all cases falls into each three 30-year periods. It is unnecessary to make a significance test to decide whether does any increase or decrease of occurrence of the daily high precipitation take place. The answer is unambiguous, it can not be verified with statistical methods.

Had we made a comparison only between the observations of the last 30-yearly period (1961–1990) and the data of the directly preceeding 30-yearly period (1931–1960), we would have come to an other conclusion (*Table 3*). In this case, we should have come to the conclusion that the difference between the percentage of the two 30-yearly periods during 1931–1990 are 6–8%.

The beginning third of the century was followed by a second 30-year period with a lot of cases of daily high precipitation. Occurrence of the daily high precipitation was less frequent in the latest 30-year period than in the beginning

Table 2. The absolute frequencies of the daily high and extremely high precipitation

Station	1901–1930					1931–1960					1961–1990				
	≥ 80 mm	≥ 70 mm	≥ 50 mm	≥ 40 mm	≥ 30 mm	≥ 80 mm	≥ 70 mm	≥ 50 mm	≥ 40 mm	≥ 30 mm	≥ 80 mm	≥ 70 mm	≥ 50 mm	≥ 40 mm	≥ 30 mm
Sopron	2	3	11	41	80	–	1	13	24	69	–	2	8	22	56
Budapest	–	–	6	15	45	1	3	3	14	53	–	1	6	12	40
Pécs	–	–	4	19	53	–	2	10	15	46	1	2	8	16	48
Szeged	–	–	2	7	33	–	–	3	19	45	–	–	5	8	32
Debrecen	–	–	3	8	26	–	–	5	15	30	1	2	10	20	47
Miskolc	1	1	13	20	48	1	1	11	22	59	–	–	3	14	44
Σ	3	4	**39**	110	285	2	7	**45**	109	302	2	7	**40**	92	267
%	–	–	**31.4**	35.4	33.4	–	–	**36.3**	35.0	35.4	–	–	**32.3**	29.6	31.2

third of the century. But the number of flash floods was much lower in the latest 30-year period (between 1961–1990) than in the period of the middle of the century (between 1931–1960).

Table 3. The absolute and relative frequencies of the daily high precipitation in Hungary

	1931–1960			1961–1990		
	≥ 50 mm	≥ 40 mm	≥ 30 mm	≥ 50 mm	≥ 40 mm	≥ 30 mm
Σ	45	109	302	40	92	267
%	53	54	53	47	46	47

4. Occurrence of the days of high precipitation

The climate data base of the Hungarian Meteorological Service gives a long series of data only for six stations. We should like to use all the raingauge observations, but those are available only from 1951 in our computerized data bank. The quantity of the data earlier used is shown in Table 1. For the six stations the summed numbers of cases with daily precipitation above 80 mm are

7, above 70 mm: 18, and above 50 mm: 124. These case numbers are not enough for further examination.

It was reasonable to rely on *Péczely*'s (1962) work, who studied the occurrence of daily precipitation above 80 mm, during 1931–1960, in all the raingauge network of Hungary. In this study the daily precipitation amounts from about 800 stations were examined for the periods of 1961–1990.

Table 4 shows the absolute frequencies specified for 10 mm intervals of the daily precipitation above 80 mm on the whole territory of Hungary during 1931–1960 (after *Péczely*) and during 1961–1990, as well. From the earlier period to the latter one, the number of cases of daily precipitation above 80 mm reduces from 521 to 417, that makes 20 percent. It seems that the decrease of the event's number appears almost uniformly at all intervals.

Table 4. The absolute frequencies specified for 10 mm intervals of the daily precipitation above 80 mm based on 800 stations in Hungary during 1931–1960 (after Péczely) and during 1961–1990

Intervals	1931–1960	1961–1990
81– 90 mm	241 cases	208 cases
91–100 mm	128 cases	101 cases
101–110 mm	56 cases	42 cases
111–120 mm	42 cases	29 cases
121–130 mm	24 cases	15 cases
131–140 mm	15 cases	6 cases
141–150 mm	5 cases	5 cases
151–160 mm	4 cases	4 cases
161–170 mm	2 cases	3 cases
171–180 mm	1 case	2 cases
181–190 mm	–	–
191–200 mm	2 cases	1 case
201–210 mm	–	1 case
...	–	–
251–260 mm	1 case	–
All cases	521 cases	417 cases

In *Table 5* the daily precipitations above 150 mm during 1961–1990 are listed. The date of 8 cases from the 11 extremes is: September 8, 1963. The date of 63 cases from the all 417 extremes during 1961–1990 is September 8, 1963, as well.

Furthermore, we introduced a new term: *the day of high precipitation above a given precipitation amount*. The definition is as follows: if the daily precipitation above a given precipitation amount (80, 70, ... or 30 mm) is observed at least at *one* station from all raingauge stations of the country, this day is referred as *high precipitation's day*. Accordingly, during the 1961–1990 period only 4 days may be named *extreme high precipitation's days above 150 mm*.

Table 5. List of the daily precipitation above 150 mm in Hungary during 1961–1990

Stations	Daily precipitation (mm)	Date
Gyömrő	203	Sep 8, 1963
Hatvan	191	Jul 27, 1963
Kartal	176	Sep 8, 1963
Mende	173	Sep 8, 1963
Apostag	168	Jul 26, 1982
Valkó	163	Sep 8, 1963
Isaszeg	162	Sep 8, 1963
Ócsa-Felsőbabád	158	Sep 8, 1963
Parádsasvár	156	Aug 3, 1974
Ócsa	154	Sep 8, 1963
Csévharaszt	151	Sep 8, 1963

In this way, the information-content of the original data significantly decreases, so that we can not say anything about all the precipitation amounts of the high precipitation's days, and the territorial extension of flash floods, respectively.

Table 6 shows the numbers of cases of daily precipitation above 30, 40, ... 150 mm, and the numbers of high *precipitation's days* above given values, during 1961–1990. The extension of rainfall above 30 mm is large enough, so it may be observed at a lot of raingauge stations. Had we did not consider the territorial extension of precipitation, the number of cases between 1961–1990 would have reduced from 36,059 to 1,991, that makes 5.5 percent. The territorial extension of the extreme high precipitations producing flash floods is smaller, so the differences between the two columns in Table 6, aren't as big as in the case of lower precipitation.

To reproduce such a table for the period of 1931–1960, after *Péczely*'s

study was impossible. But *Péczely* had made the data independent from the density change of raingauge stations. This gave possibility to ascertain the number of days called *extreme high precipitation's days above 80 mm* during 1931-1960 based on his figure, that is 162.

The number of extreme high *precipitation's days* above 80 mm is 167 during 1961–1990. Consequently, had we disregarded the territorial extension of precipitation, and had we examined only its frequency distribution in country, we would have established more occurrence of extreme high precipitation's day above 80 mm in the latest 30-yearly period (between 1961–1990) than in the middle period of the century (between 1931–1960).

Table 6. The absolute frequencies of the number of all cases of daily precipitation and the number of precipitation's days above 30 mm in Hungary during 1961–1990

Threshold (mm)	Cases	Precipitation's days
> 30	36,059	1,991
> 40	12,840	1,223
> 50	5,010	763
> 60	2,034	457
> 70	897	273
> 80	**417**	**167**
> 90	209	95
> 100	108	54
> 110	66	31
> 120	37	14
> 130	22	6
> 140	16	5
> 150	11	4

We have come to the conclusions based on results in Table 4 that the number of cases of daily extreme high precipitation above 80 mm reduces by 20 percent (from 521 to 417), and after aforesaid establishments that the occurrence of extreme high *precipitation's day* above 80 mm grows from 162 to 167. But these deviations are not considerable. Furthermore, it can be said that *the occurrence of the daily high and extreme high precipitation in Hungary during the 20th century does not show a decrease or an increase which would exceed the natural climate variability.*

5. Annual variation of the daily high precipitation

Our further examination is directed to the annual variation of the daily high precipitation. We have examined its monthly frequency occurrences. The relative frequencies of monthly occurrence of the daily extreme high precipitation above 80 mm are shown in *Fig. 1*, between 1931–1960 (after *Péczely*) and 1961–1990 according to our investigation. Fig. 1 also indicates the relative frequencies of numbers of all cases (527 and 417 cases). The 70 percent of the daily extreme high precipitation (examined by *Péczely*) has fallen in June-July, and its 93 percent in May-August, between 1931–1960. Their annual variation distorts towards the left, it suddenly rises and slowly damps. The annual variation of the daily extreme high precipitation in the period of 1961–1990 shows symmetry: more than half of all cases occurred in July-August (nearly at the same rate), and 93 percent was found in 4 months, from June to September. It seems that in the annual variation of the daily high precipitation there is one-monthly discrepancy. However, we have to consider that data of all observations are taken into account, for example September 8, 1963 is included when 63 stations reported extreme precipitation.

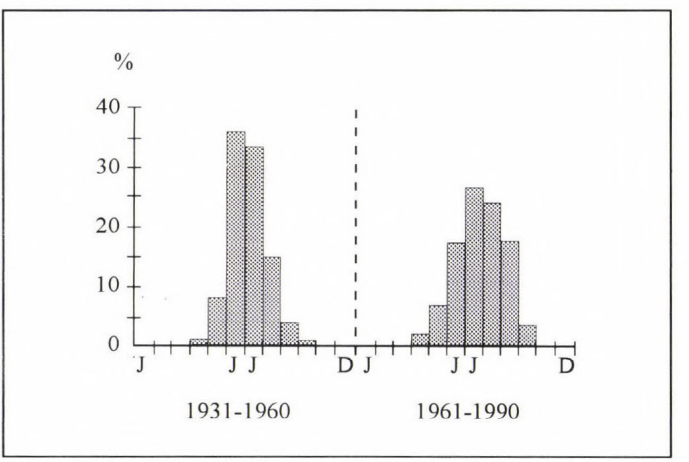

Fig. 1. The relative frequencies of monthly occurrence of the daily extreme high precipitation above 80 mm in Hungary during 1931–1960 (after *Péczely*) and 1961–1990 (present study).

Fig. 2 shows the relative frequencies of monthly occurrence of the *precipitaton's days* above 50, 60, 70, 80, 90 and 100 mm, between 1961–1990. Here, the extreme precipitation amounts observed in the same days on several stations have not been taken into account with multiple weight. In Fig. 2 the maxima of the histograms fall in July-August, and they represent a greater

frequency with increasing of extremity. So, we can conclude that there is a change in timing of maximum of the frequency occurrence of the daily extreme high precipitation from early summer to the second half of summer. This change of annual variation can be related to the appearance of the seasonal change.

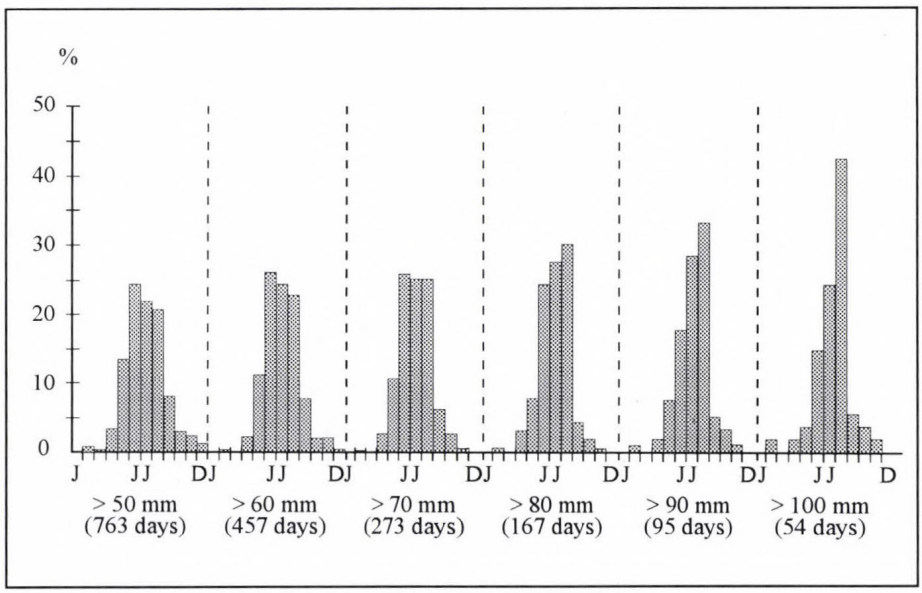

Fig. 2. The relative frequencies of monthly occurrence of the precipitation's days above various thresholds in Hungary during 1961–1990.

Acknowledgements—The author wishes to thank *T. Tänczer* for revising this manuscript. This paper was supported by contract OTKA-443 with the Hungarian Academy of Sciences.

References

Faragó, T., Iványi, Zs. and *Szalai, S.* (eds.), 1990, 1991: Climate variability and change, Vol. I., Vol. II. (in Hungarian). Környezetvéd. és Területfejl. Min., Orsz. Meteorológiai Szolgálat, Budapest.

Mika, J., 1991: Regional features of a stronger global warming over Hungary (in Hungarian). *Időjárás 95*, 265-278.

Mika, J., 1993: Effects of the large-scale circulation on local climate anomalies in relation to GCM outputs. *Időjárás 97*, 21-34.

Péczely, G., 1962: Frequency of the daily precipitation above 80 mm in Hungary (in Hungarian). *Időjárás 66*, 197-204.

Schirok-Kriston, I., 1983: Frequency analysis of storm rainfalls and estimation of the probable maximum precipitation (in Hungarian). Vízügyi Közlemények LXV., 167-187.

BOOK REVIEWS

Frakes, L. A., Francis, J. E. and *Syktus, J. I.:* **Climate Modes of the Phanerozoic**. Cambridge University Press, 1992. pp. 272, 11 chapters.

This book first describes, in a concise way, the salient features of Earth climates over the last 600 mil. years. With this background information in hand its purpose is to recognize and then compare similar climatic states in history. So the changes in the Earth's climate from the Cambrian (partly late Precambrian as well) to Quaternary come under scrutiny in this book. Geological evidence for ancient climates is examined, such as the distribution of climate-sensitive sediments, including coals, evaporites, and glacial deposited.

The Earth's climate has changed many times throughout the Phanerozoic. Thus in this book the climate history has been divided into Warm and Cool Modes, intervals when either the Earth was in a 'greenhouse' state with higher levels of atmospheric CO_2 and polar regions free of ice, or the global climate was cooler and ice was present in high latitudes.

The Cool Modes are defined as times of global refrigeration during which the polar regions were covered by large permanent ice caps or when the high-latitude regions were only seasonally sufficiently cold for the formation of ice during winter. The record of ancient glaciations, represented by such well-known features as tillites, striated pavements, is not difficult to confirm.

The Warm Modes are defined as times when climates were globally warm, as indicated by abundance of evaporites, geochemical data, faunal distribution, and little or no polar ice. As more climate data are collected in future, it may be shown that these divisions into climate modes are far too simple or completely wrong—write the authors. Because these Modes span rather long intervals of approximately 150 mil. years, they do include brief intervals of contrasting climates.

What are the causes of climate change? The studies presented here highlight the complex interactions between the carbon cycle, continental distribution, tectonics, sea level variations, ocean circulation and temperature change as well as other parameters. In particular, the potential of the carbon isotope records as an important signal of the past climates of Earth is explored.

The book consists of eleven, most of them describing the Warm and Cool Modes in chronological order. At the end of the book, there are approximately 850 references, but excluding such authors as *M. Schwarzbach, W. Köppen, A. Wegener, H. Lamb* and others.

G. Koppány

Houghton, J.: **Global Warming. The Complete Briefing.** Lion Publishing, Oxford, 1994. pp. 192, 12 chapters.

Sir John Houghton, the author of this book, is co-chairman of the Science Assessment Working Group of the Intergovernment Panel on Climate Change (IPCC), chairman of the Royal Commission on Environmental Pollution, and a member of the British Government's Panel on Sustainable Development. Besides: his name is well-known in meteorological literature, he has published a great number of excellent books and papers.

The book consists of twelve chapters, a very useful and up to date glossary including references to UN Conference on Environment and Development at Rio de Janeiro in June 1992, and an index. Perhaps the most important initiatory facts of writing this book have been as follow.

For the Earth as a whole, seven of eight warmest years on record have occurred in the 1980-s and early 1990-s. The storm which swept western Europe in October 1987 was the worst in the area since 1703. In 1988 the highest flood levels recorded affected 80 per cent of Bangladesh.

There is a consensus among the world scientific community about the fact of global warming, but there is fierce debate about the scale of the problem and what, if anything, should be done about it. This important new book—the most comprehensive work ever written on the subject for a non-specialist readership—moves no debate on.

The author explores the whole theory of global warming and sets out the findings of the world scientific community. His clear exposition of current scientific understanding, including the uncertainties, provides a balanced account which will be welcomed by students and general readers alike. The author uses the latest research to investigate the likely consequences of the world's current course if no action would be taken.

This book addresses the questions that lie at the heart of political and social concern about the environment. Is the current lifestyle of modern, industrial society sustainable? What kind of world will our grandchildren inherit?

G. Koppány

NEWS

Joint Meeting on Global Atmospheric Chemistry

The Commission on Atmospheric Chemistry and Global Pollution (CACGP) of the International Association of Meteorology and Atmospheric Physics and the International Global Atmospheric Chemistry Project (IGAC) of the International Geosphere-Biosphere Programme held a joint conference in Fuji-Yoshida (Japan) between September 5 and 9, 1994. This was the 8th regular conference of CACGP, while the meeting was the second in a series initiated by IGAC. The host organization was the Department of Earth and Planetary Physics of the University of Tokyo headed by *T. Ogawa*. Into the conference program (chairman of the Program Committee: *S. A. Penkett, U.K.*) the following sessions were included: (1) Greenhouse Gases; (2) Tropospheric Ozone; (3) Sulfur and Nitrogen Cycles; and (4) Aerosol and Cloud Chemistry. While many lectures were given orally, the major part of the papers was presented on posters.

The lectures of the first session made it clear that the global concentration of some greenhouse gases has decreased or at least it has been stabilized during the last years. This very important fact is observed mainly in the level of methane, carbon monoxide and some freons. It was a great discussion, without final conclusions, about the possible reasons for these observations. Thus, it was proposed that this phenomenon is due to the decrease of emissions, to changes in oxidation capacity of the atmosphere or to the modifications of global atmospheric circulation. Many new observational facts were presented at the conference on tropospheric ozone. These measurements were carried out in areas where our knowledge was rather poor like the North Atlantic, South Atlantic and several African regions. These latter programs were mainly made to gain further evidences concerning the effects of biomass burning on the ozone formation in the troposphere.

The session on sulfur and nitrogen cycles was mainly devoted to problems (e.g. acidity) in Asia and to the role of oceanic biogenic sulfur emission in the control of the global sulfur budget. Some new precipitation chemistry data were discussed, based on samplings in Asian regions (e.g. Siberia, Thailand) not yet studied. Among other things the main aim of the last session was to evaluate the possible role of anthropogenic aerosol particles in the climate variations. It was concluded that sulfate particles caused by fossil fuel burning will regionally reduce the effects of man-made greenhouse gases in industrialized areas (north-eastern part of North America, Europe and China). Further research is needed, however, to confirm this conclusion.

The organization of the conference was excellent. About 250 participants from all over the world enjoyed not only the scientific presentations—partly from high levelled Japanese scientists—, but also the beautiful environment of the Fuji mountain and the warm Japanese hospitality. It was a good decision to hold for the first time the conference of CACGP outside Europe and North America.

At the conference it was announced that the next scientific meeting of CACGP will take place in Seattle, Washington (U.S.A.) during 1998. Finally, one has to note that new officers and members were elected by CACGP. The new president is *I. Galbally* (Australia), while the commission secretary is *L. A. Barry* (Canada).

E. Mészáros

ATMOSPHERIC ENVIRONMENT

an international journal

To promote the distribution of Atmospheric Environment *Időjárás* publishes regularly the *contents* of this important journal. For further information the interested reader is asked to contact *Dr. P. Brimblecombe,* School for Environmental Sciences, University of East Anglia, Norwich NR 7TJ, U.K.

Volume 28 Number 7 1994

Volume 28 Number 8 1994

The Glen E. Gordon Memorial Issue

A.E. Sheffield, G.E. Gordon, L.A. Currie and *G.E. Riederer*: Organic, elemental, and isotopic tracers of air pollution sources in Albuquerque, NM, 1371-1384.

Xudong Huang, I. Olmez, N.K. Aras and *G.E. Gordon*: Emissions of trace elements from motor vehicles: potential marker elements and source composition profile, 1385-1391.

M.S. Germani and *W.H. Zoller*: Solubilities of elements on in-stack suspended particles from a municipal incinerator, 1393-1400.

D.L. Anderson, M.E. Kitto, L. McCarthy and *W.H. Zoller*: Sources and atmospheric distribution of particulate and gas-phase boron, 1401-1410.

D.M. Glover and *P.K. Hopke*: Exploration of multivariate atmospheric particulate compositional data by projection pursuit, 1411-1424.

M.P. Zelenka, W.E. Wilson, J.C. Chow and *P.J. Lioy*: A combined TTFA/CMB receptor modeling approach and its application to air pollution sources in China, 1425-1435.

Y. Hashimoto, Y. Sekine, Hui Kang Kim, Zong Liang Chen and *Zhi Min Yang*: Atmospheric fingerprints of East Asia, 1986-1991. An urgent record of aerosol analysis by the JACK Network, 1437-1445.

Ning Gao, Meng-Dawn Cheng and *P.K. Hopke*: Receptor modeling of airborne ionic species collected in SCAQS, 1447-1470.

Zhong Yu Wu, Ming Han, Zhi Chao Lin and *J.M. Ondov*: Chesapeake Bay atmospheric deposition study, Year 1: sources and dry deposition of selected elements in aerosol particles, 1471-1486.

J.R. Scudlark, K.M. Conko and *T.M. Church*: Atmospheric wet deposition of trace elements to chesapeake Bay: CBAD Study Year 1 results, 1487-1498.

D.L. Leister and *J.E. Baker*: Atmospheric deposition of organic contaminants to the Chesapeake Bay, 1499-1520.

E.G. Burkhard, V.A. Dutkiewicz and *L. Husain*: A study of SO_2, SO_4^{2-} and trace elements in clear air and clouds above the midwestern United States, 1521-1533.

G.J. Keeler and *W.R. Pierson*: Regional trace element and sulfate transport, 1535-1548.

N.Z. Heidam: Arctic aerosol factor models: validation by marginally detected elements, 1549-1555.

F.A. Akeredolu, L.A. Barrie, M.P. Olson, K.K. Olkawa, J.M. Pacyna and *G.J. Keeler*: The flux of anthropogenic trace metals into the Arctic from the mid-latitudes in 1979/80, 1557-1572.

Volume 28 Number 9 1994

A. Malyschew, H.-J. Schmidt, K.G. Weil and *P. Hoffmann*: Methods for characterization of colloid particles in rain water, 1575-1581.

H. Skov, Th. Benter, R.N. Schindler, J. Hjorth and *G. Restelli*: Epoxide formation in the reactions of the nitrate radical with 2,3-dimethyl-2-butene, *cis*- and *trans*-2-butene and isoprene, 1583-1592.

R.M. Harrison, M.I. Msibi, A.-M. N. Kitto and *S. Yamulki*: Atmospheric chemical transformations of nitrogen compounds measured in the North Sea Experimental, September 1991, 1593-1599.

A.C. Comrie: A synoptic climatology of rural ozone pollution at three forest sites in Pennsylvania, 1601-1614.

I.Y. Lee and *H.M. Park*: Comparison of microphysics parameterizations in a three-dimensional dynamic cloud model, 1615-1625.

S. Kutsuna, M. Kasuda and *T. Ibusuki*: Transformation and decomposition of 1,1,1-trichloroethane on titanium dioxide in the dark and under photoillumination, 1627-1631.

R. Bellasio and *M. Tamponi*: MDGP: a new Eulerian 3D unsteady state model for heavy gas dispersion, 1633-1643.

S. Loranger and *J. Zayed*: Manganese and lead concentrations in ambient air and emission rates from unleaded and leaded gasoline between 1981 and 1992 in Canada: a comparative study, 1645-1651.

Volume 28 Number 10 1994

Volume 28 Number 11 1994

5th International Wind and Water Tunnel Dispersion Modelling Workshop, 30 October–1 November, 1991, Warren Spring Laboratory, Stevenage, U.K.

Volume 28 Number 12 1994

Volume 28 Number 13 1994

The Kuwaiti Oil Fires

Short Communication

NOTES TO CONTRIBUTORS

The purpose of *Időjárás* is to publish papers in the field of theoretical and applied meteorology. These may be reports on new results of scientific investigations, critical review articles summarizing current problems in certain subject, or shorter contributions dealing with a specific question. Authors may be of any nationality but papers are published only in English.

Papers will be subjected to constructive criticism by unidentified referees.

* * *

The manuscript should meet the following formal requirements:

Title should contain the title of the paper, the names(s) of the author(s) with indication of the name and address of employment.

The title should be followed by an *abstract* containing the aim, method and conclusions of the scientific investigation. After the abstract, the *key-words* of the content of the paper must be given.

Three copies of the manuscript, typed with double space, should be sent to the Editor-in-Chief: *P.O. Box 39, H-1675 Budapest,* Hungary.

References: The text citation should contain the name(s) of the author(s) in Italic letter or underlined and the year of publication. In case of one author: *Miller* (1989), or if the name of the author cannot be fitted into the text: *(Miller,* 1989); in the case of two authors: *Gamov* and *Cleveland* (1973); if there are more than two authors: *Smith et al.* (1990). When referring to several papers published in the same year by the same author, the year of publication should be followed by letters a,b etc. At the end of the paper the list of references should be arranged alphabetically. For an article: the name(s) of author(s) in Italics or underlined, year, title of article, name of journal, volume number (the latter two in Italics or underlined) and pages. E.g. *Nathan, K. K.,* 1986: A note on the relationship between photosynthetically active radiation and cloud amount. *Időjárás 90,* 10-13. For a book: the name(s) of author(s), year, title of the book (all in Italics or underlined with except of the year), publisher and place of publication. E.g. *Junge, C. E.,* 1963: *Air Chemistry and Radioactivity.* Academic Press, New York and London.

Figures should be prepared entirely in black India ink upon transparent paper or copied by a good quality copier. A series of figures should be attached to each copy of the manuscript. The legends of figures should be given on a separate sheet. Photographs of good quality may be provided in black and white.

Tables should be marked by Arabic numbers and provided on separate sheets together with relevant captions. In one table the column number is maximum 13 if possible. One column should not contain more than five characters.

Mathematical formulas and *symbols:* non-Latin letters and hand-written marks should be explained by making marginal notes in pencil.

The final text should be submitted both in manuscript form and on *diskette.* Use standard 3.5" or 5.25" DOS formatted diskettes for this purpose. The following word processors are supported: WordPerfect 5.1, WordPerfect for Windows 5.1, Microsoft Word 5.5, Microsoft Word for Windows 2.0. In all other cases the preferred text format is ASCII.

* * *

Authors receive 30 *reprints* free of charge. Additional reprints may be ordered at the authors' expense when sending back the proofs to the Editorial Office.

Published by the Hungarian Meteorological Service

Budapest, Hungary

INDEX: 26 361

HU ISSN 0324-6329